
1 November 2016

To: ORCAS data-processing file
FROM: Al Cooper
SUBJECT: vertical wind for ORCAS

1 The problem in ORCAS

The standard processing for vertical wind did not work well for ORCAS. The flights featured frequent climbs and descents, with some low-level flight, and the vertical-wind measurements seemed to correlate with climbs and descents in ways that were hard to understand. The study of the radome was complicated by the absence of any speed runs except for a single one on test flight 1, 2242–2256, which only covered a limited speed range.

Apparent systematic effects during low-level flight and especially during climbs seemed to point to some difference in performance of the radome during some periods of flight. It appeared plausible that these periods were linked to the use of flaps, which could conceivably affect the airflow in ways that change the sensitivity coefficients of the radome. This will be explored further after an initial application of the standard approach to indicate why there appears to be a problem with that approach.

2 The standard fit

The first step here will be to re-fit the measurements to the standard formula used to represent angle of attack α , from the Processing Algorithms technical note:

$$\alpha = c_0 + \frac{\Delta p_\alpha}{q} (c_1 + c_2 M) \quad (1)$$

where Δp_α is the pressure difference between upward and downward ports on the radome (AD-IFR), q is dynamic pressure (QCF), and M is the Mach number calculated using the uncorrected static and dynamic pressure (PSF and QCF). The three coefficients specified in that document are $\{c\} = \{4.605, 18.44, 6.75\}$. The approach used here is described in detail in the Wind Uncertainty technical note. It is to use a reference value for angle of attack, α^* , defined by

$$\alpha^* = \theta - \frac{w_p}{V} \quad (2)$$

which would equal the angle of attack if the vertical wind were zero, and then determine the coefficients in (1) that minimize the difference between α^* and α .

3 Data used

This memo will use measurements from rf01–rf19, excluding rf12 for which the netCDF file was not usable in the version I downloaded from /scr/raf_data/ORCAS (downloaded about 12 Oct 2016). Some data restrictions are needed, for two reasons:

1. Near the start and end of flights, there are periods where flaps and/or landing gear are deployed, leading to large potential errors in angle of attack. For ORCAS, there are frequent descents to low level followed by climbs, so it is best to exclude periods of low-speed flight unless at levels well above the surface where they may have arisen in the course of speed runs. (There were none during regular research flights in ORCAS.) It appears that if TASX is required to exceed 110 m/s, this provides some separation between these two cases, so that will be used to qualify data for this study,. For most other projects, 130 m/s was used, but in ORCAS there are many near-ocean legs flown slower than this so 110 m/s appears more appropriate.
2. Because there are additional potential uncertainties for measurements in turns, the data used to determine sensitivity coefficients in the following were restricted to cases where the roll was between -2 and 2° . This is also needed for the reference value developed below for angle-of-attack to be valid.
3. There seemed to be more scatter present for flights 5, 10, 13, 15 and 16, so those flights were omitted from some composite compilations of data to avoid possible distortion of results by regions where measurements appear questionable.

4 New coefficients

4.1 The standard formula with new coefficients

A fit of (1) to the data from flight 6 only, qualified as in Sect. 3, led to best-fit coefficients $\{c_{1\dots 3}\} = \{4.427, 18.563, 3.605\}$. A comparison of the angle of attack produced by (1) with these coefficients to the reference values given by (2) is shown in Fig. 1. While the representation of the variation in reference angle is reasonable, there are some regions with significant scatter from the fit and a pattern with calculated values larger than the reference values at high angle of attack that is not represented well by the fit. A histogram of the difference (Fig. 2) shows a reasonable distribution but a second peak where the fitted angle-of-attack is about 0.1° higher than the reference value. The residual standard deviation for this fit, 0.096° , was reasonable but affected by that second peak. The standard deviation was reduced only slightly (by about 10%) from the fit that used only the first term, but it still appears worthwhile to use this three-coefficient fit instead. Several other options were considered, including direct dependence on Mach number, air density, pressure, altitude, and powers and products of these, but none of these provided significant (>0.01) further reduction in the standard deviation of the residuals. Two added terms that did give significant reduction were

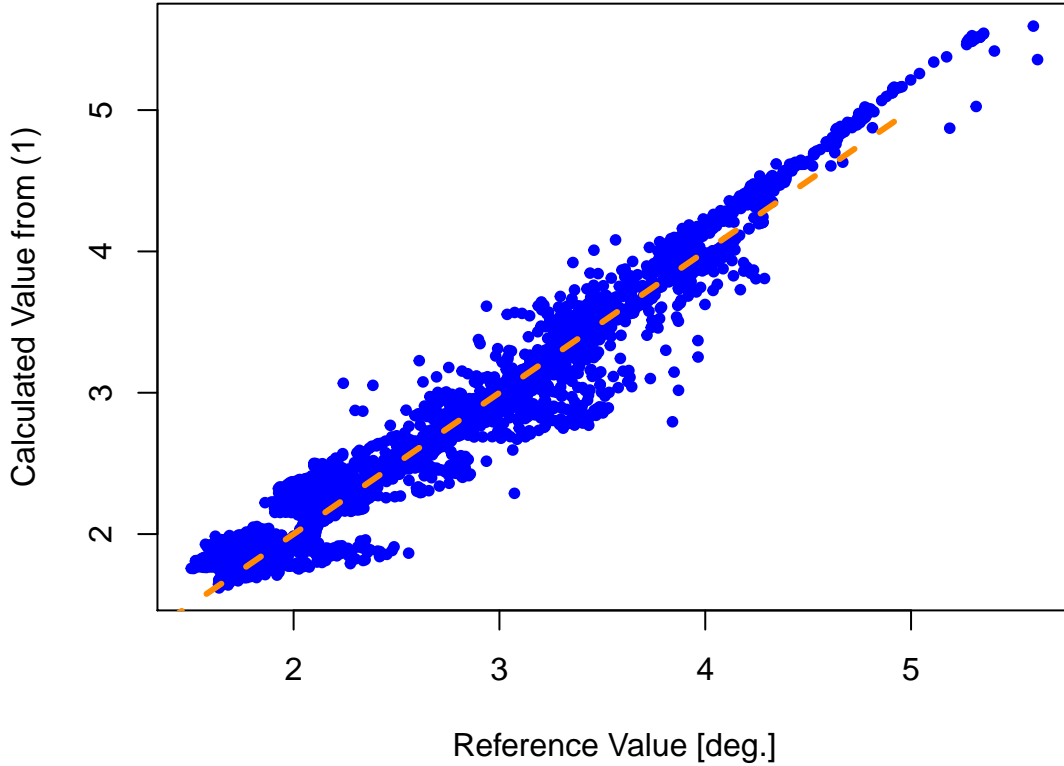


Figure 1: Calculated value of angle of attack vs the reference value used in the fit.

q (QCF) and z (GGALT) or $\log(z)$. These are discussed in the next section and do provide some improvement in the residual standard deviation and in plots like Figs. 1 and 2.

```
## lm(formula = AOAREF ~ QR + I(QR * M), data = DF)
## [1] "Coefficients:"
##              Estimate Std. Error t value Pr(>|t|)
## (Intercept)   4.43     0.00204 2169.8 0.00e+00
## QR           18.56     0.07092   261.7 0.00e+00
## I(QR * M)      3.61     0.09673    37.3 1.97e-292
## [1] "Residual standard deviation: 0.096, dof=17149"
## [1] "R-squared 0.975"
```

The revised vertical wind based on the new three-coefficient fit can be estimated from the previous value (WIC) modified to be $WIX=WIC+(\alpha \cdot AKRD)\pi V/180$ where α is given by (1), V is the

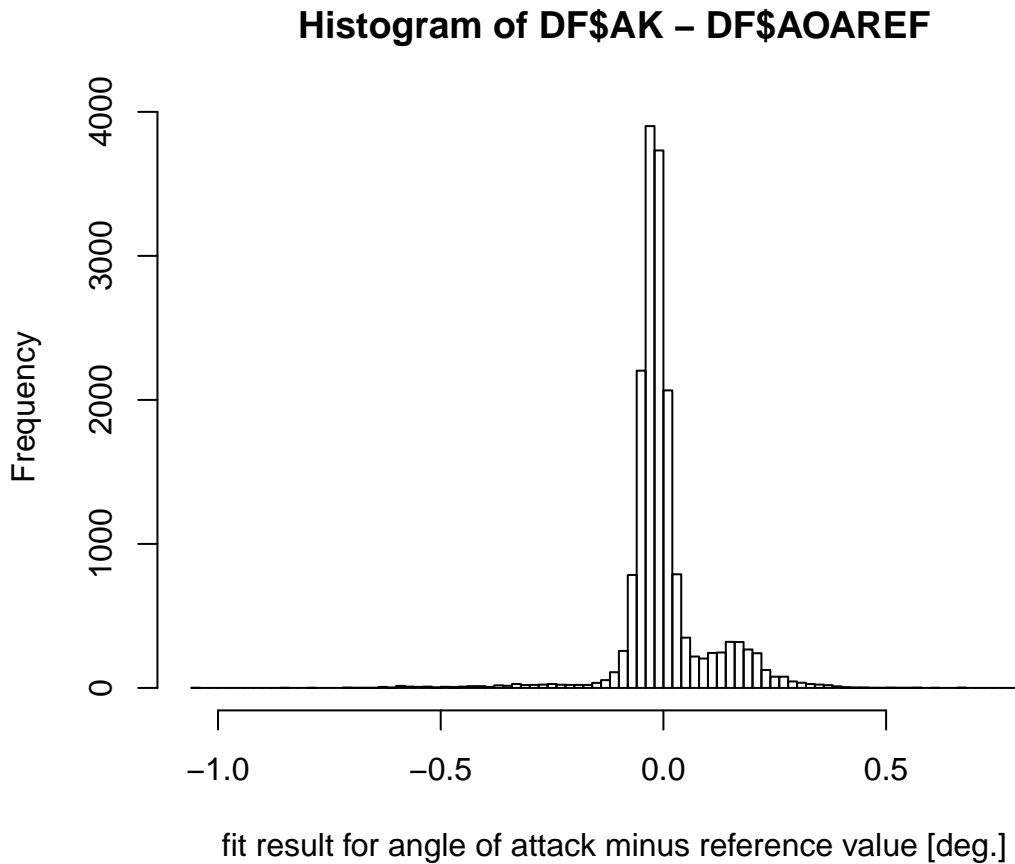


Figure 2: Histogram of the difference between the calculated angle of attack and the reference value.

airspeed and $\pi/180$ is needed to convert from degrees to radians. Figure 3 shows the result for flight 6 with the addition of this new measurement of the vertical wind. The red trace (WIXS, WIX with 60-s smoothing) represents the new variable. Both WIC and WIX have clear problems during the period from about 20:00:00 to 21:00:00 UTC, a period when the flight descended from high level to near the surface and then climbed back to the original height. These problems were not eliminated by the inclusion of the additional terms QCF and GGALT in the fit, although there was some reduction in the apparent errors. These apparent errors, which appear associated with flight below about 30,000 ft, point to some remaining problem with the results. The added complexity of the extra terms does not resolve the problem, so a different approach seems needed..

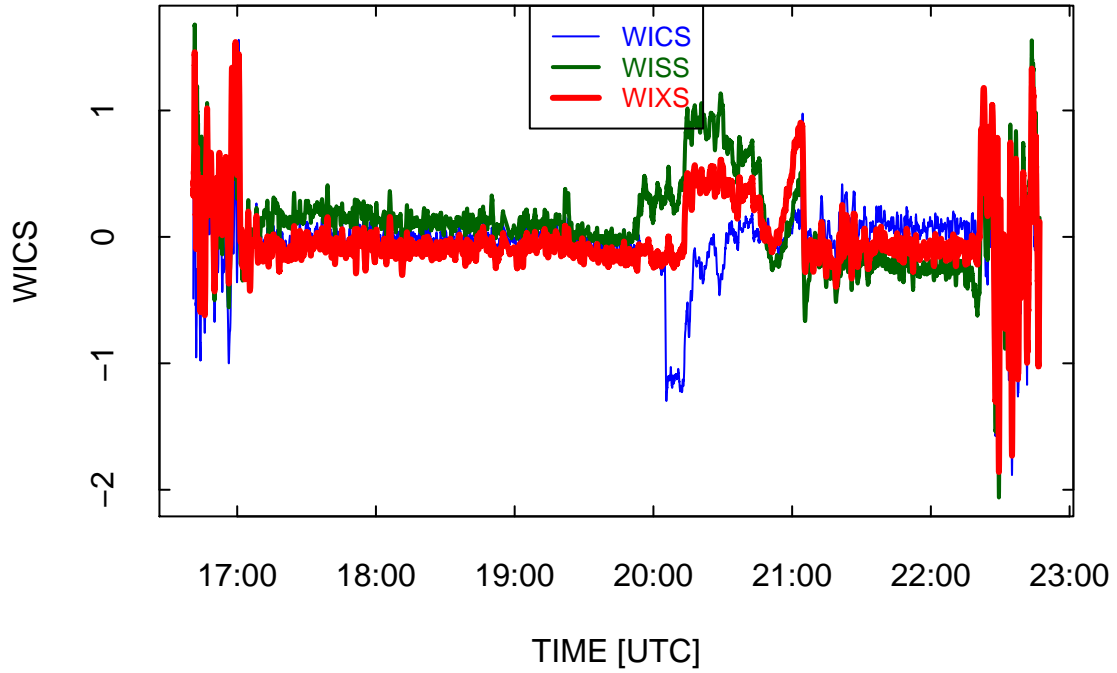


Figure 3: Vertical wind measurements for ORCAS flight 6. WICS is the original vertical wind in the EOL directory for ORCAS, WISS is the vertical wind calculated using the standard sensitivity coefficients in the document on processing algorithms, and WIXC is the vertical wind based on the new three-coefficient fit. All have been smoothed (about 20-s time constant) to reduce scatter over this plot, which spans the full flight.

4.2 Consideration of aerodynamic effects

It seems unlikely that there were real vertical wind values of the magnitude of these measurements, so it is worthwhile to look for sources of these errors. Perhaps the radome sensitivity to angle of attack is different in climbs and descents, the measured rate-of-climb of the aircraft might be in error, or there might be timing errors among the measurements. However, preliminary checks make these appear unlikely,. It seems more likely that the error arises from some sensitivity to performance characteristics of the aircraft, like deployment of flaps or spoilers and/or changes in thrust. There is no record of when flaps are deployed and to what degree, and there is similarly no record of engine thrust, but some of the apparently erroneous measurements occur at times when it is reasonable that partial flaps might be used and/or when there are significant changes in engine power.

To investigate the latter possibility, a new term was introduced that should characterize the perfor-

mance and might correlate with the observed errors, as follows: The lift L generated by an airfoil is expected to depend on a coefficient of lift c_L , the air density ρ_a , the airspeed V , and a representative surface area A , according to:

$$L = \frac{1}{2} \rho_a V^2 c_L A \quad (3)$$

and in turn the coefficient of lift depends approximately linearly on the angle of attack α , although this angle of attack may be offset from the standard value relative to the aircraft longitudinal axis. The relationship and reference angle for angle-of-attack may change when flaps are deployed so it might be expected that $c_L = c_0(\alpha - \alpha_0)$ where c_0 and α_0 both change with flap deployment. The factor $c_L A$ therefore changes with changes in aircraft configuration. The lift will normally be matched approximately to the weight of the aircraft except during short periods of vertical acceleration at the start and end of climbs and descents.¹ If the weight of the aircraft is W then it would be expected that

$$c_L A = \frac{2W(t)}{\rho_a V^2} = \frac{W(t)}{q} \quad (4)$$

where $q = \rho_a V^2 / 2$ is the dynamic pressure, so if K is defined to be

$$K = \frac{aW(t)}{q} \quad (5)$$

(where the factor $a = 500/W_0$ is introduced for plotting convenience and the weight $W(t)$ is taken to be $W_0 - R_f(t - t_0)$ with W_0 the takeoff weight at time t_0 and R_f the rate of fuel burn, taken here to be about 0.85 lb/s)² it would be expected that K is proportional to $c_L A$ and so will change when the aircraft configuration changes. Some of the ORCAS flights are quite short and likely started with less than full fuel, so it may be a better approximation to assume a landing weight instead. Representative numbers (needing refinement by consultation with pilot's records) might be $W_0 = 80,000$ or, alternately, $65,000 + R_f(t_f - t_0)$ with t_f the time of landing.

For normal flight (without flaps or speed brakes) A would be constant and the coefficient of lift would vary linearly with α^* , leading to a region in a plot of K vs. α^* with a linear relationship. For normal flight, a scatterplot of these variables shows that they can be regarded as linearly related without offset, approximately according to the relationship $K = 1.5\alpha^*$. Figure 4 shows that the ratio departs significantly from 1.5 during parts of the flight, including the initial climb and final descent and the period from about 19:45:00 to 21:00:00 UTC when there was a descent to near the surface, a brief period of level flight, and then a climb back to the original altitude. The value of K/α^* is lower than 1.5 for that intermediate period, while it might be expected to be

¹A first-order correction would be $L(1 + \gamma^2) = W$ where $\gamma = \arctan(w_p/V)$ with w_p the rate of climb and V the airspeed.

²A better estimate would consider variations in this fuel burn rate during climbs and descents and with aircraft weight, but this is a reasonable first estimate. The python program "PlanFlight.py" incorporates better estimates of the rate of fuel burn.

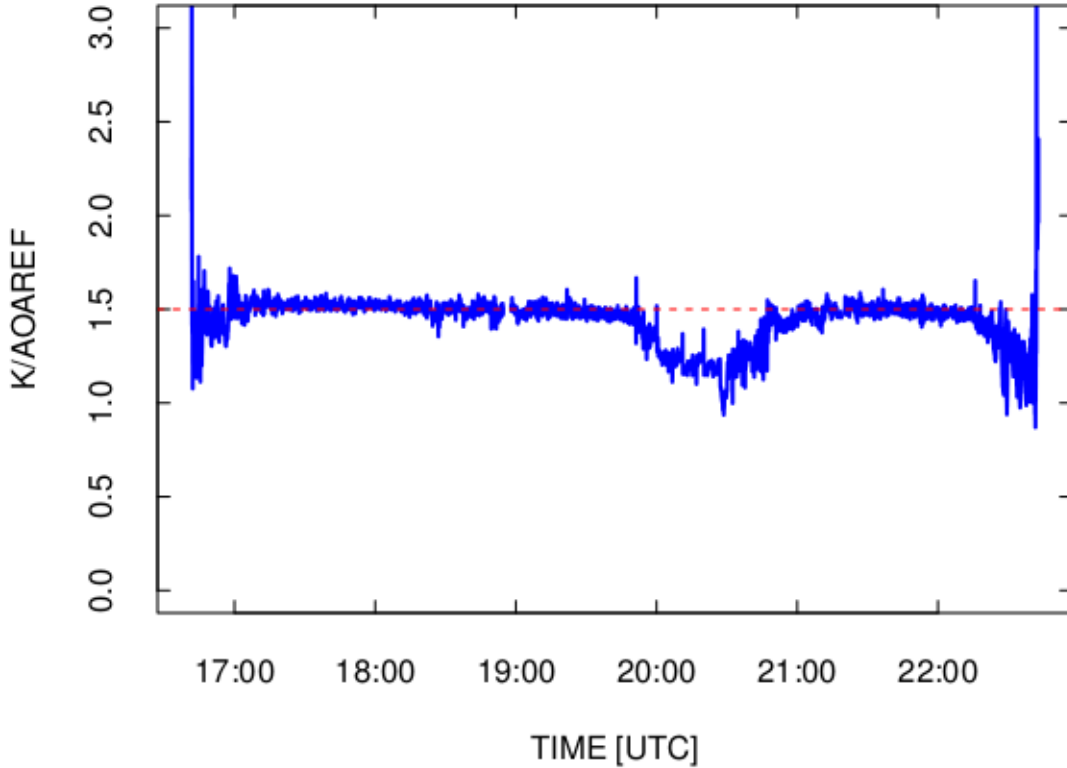


Figure 4: Ratio of K to α^* for ORCAS flight 6. The dashed-red line is a reference line at the value 1.5 for the ratio.

higher because both the coefficient of lift and the effective lifting surface area increase if flaps are deployed. The result can still be lower if the flaps or spoilers cause an offset in the effective angle of attack affecting the lifting surface, which is different from α^* because α^* is measured relative to the longitudinal axis of the aircraft rather than the chord of the wings. At the start and end of the flight, there are periods where K/α^* has high values, presumably because full flaps are deployed here. (Airspeeds less than 85 m/s are excluded from these plots to avoid inclusion of points while the aircraft is still on the runway.)

Figure 5 shows the distribution of values of K/α^* for this flight, and Fig. 6 shows the values of K plotted vs. values of α^* (with short periods at the start and end excluded to avoid regions with full flaps), with colors separating the “normal” from “possible flaps” regions of flight. If values of K/α^* larger than 1.45 are assumed to be “normal” flight, this provides a way of including only these points when determining the sensitivity coefficients. Figure 7 shows the height of the aircraft during ORCAS flight 6, with blue indicating normal flight and red indicating times when the

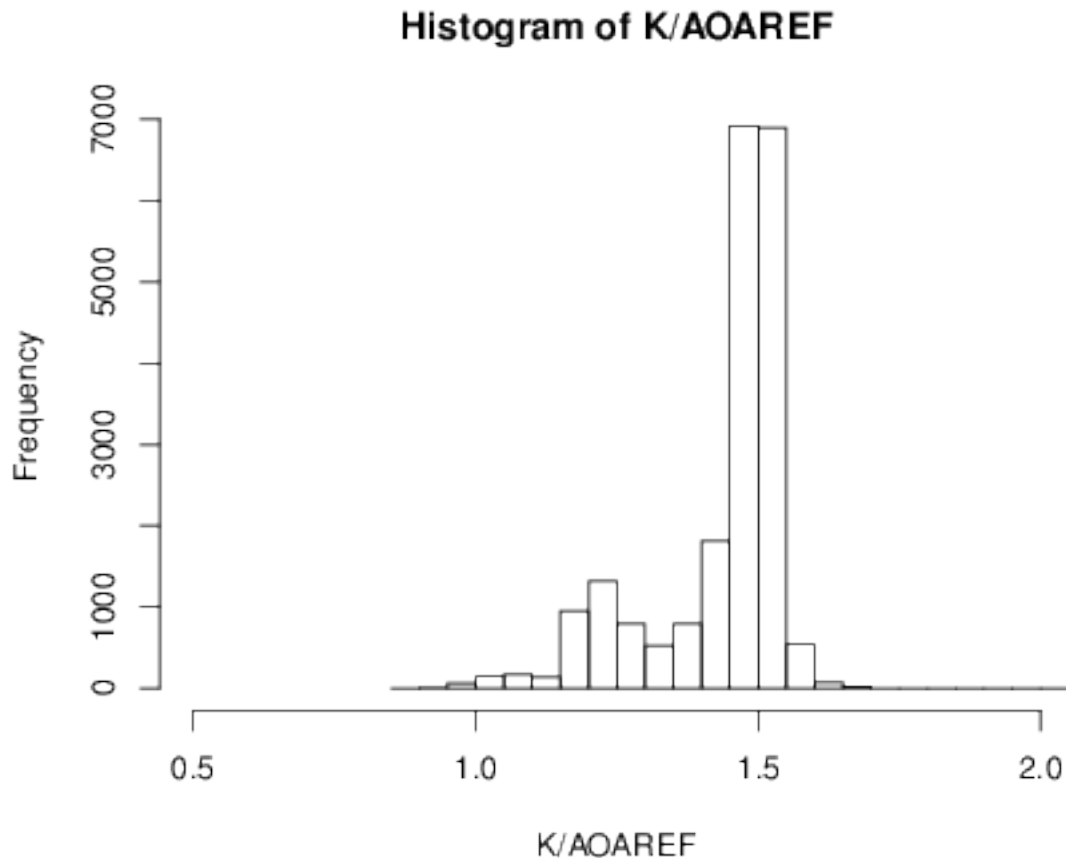


Figure 5: histogram of K/α^* for ORCAS flight 6.

aircraft configuration may affect the coefficient of lift and the airflow around the aircraft. The red portions are in reasonable correspondence with times when the aircraft configuration might change and also correlate reasonably to those times when the vertical wind appears to be erroneous.

```
## lm(formula = AOAREF ~ QR + I(QR * M) + QCF + I(log(GGALT)), data = DF)
## [1] "Coefficients:"
##                               Estimate Std. Error t value Pr(>|t|)
## (Intercept)      4.55529   3.49e-03 1304.6 0.00e+00
## QR              17.18537   2.62e-02   655.2 0.00e+00
## I(QR * M)       2.54404   3.58e-02    71.0 0.00e+00
## QCF             -0.00371   2.05e-05  -180.7 0.00e+00
## I(log(GGALT))  0.00978   3.38e-04     28.9 1.38e-183
## [1] "Residual standard deviation: 0.112, dof=196448"
## [1] "R-squared 0.953"
```

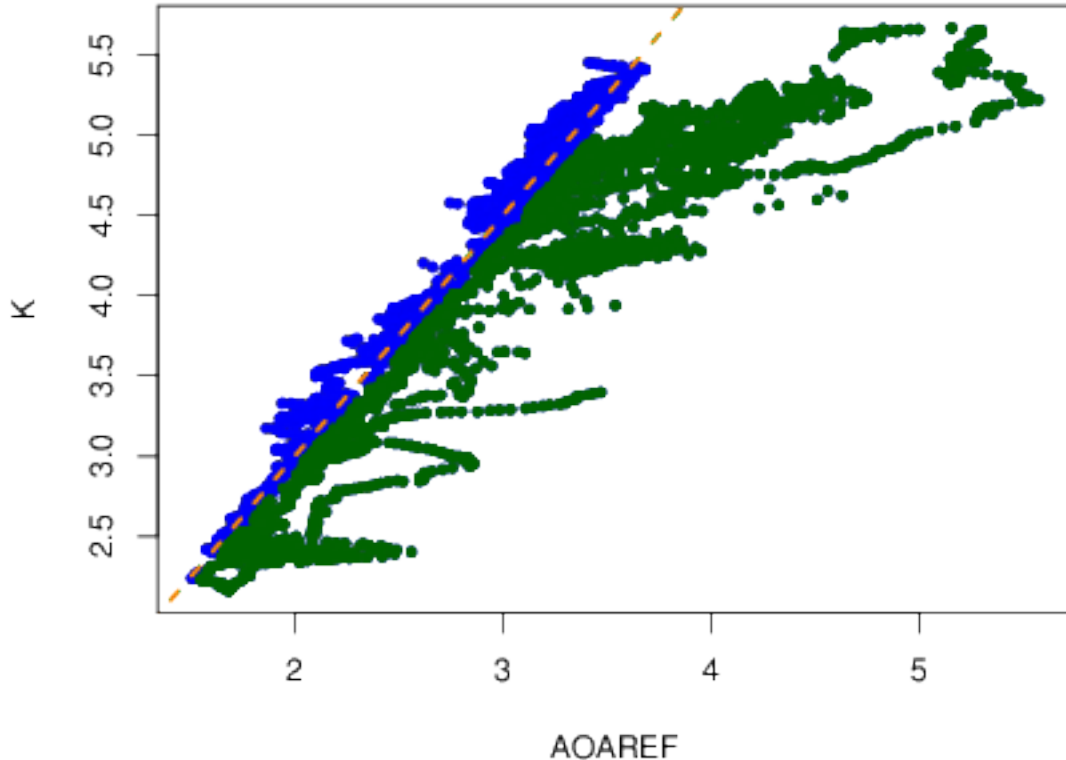


Figure 6: Values of K as a function of α^* for ORCAS flight 6. Points with $K/\alpha^* < 1.45$ are shown as green symbols and other points (representing "normal" flight) as blue symbols. The dashed orange line corresponds to $K = 1.5\alpha^*$.

Because K depends on $1/q$, this suggests that an improved fit might be obtained by including the variable QCF in the empirical representation of angle of attack. When this was tested, there was a significant improvement in the fit, with a linear rather than inverse dependence providing lower residual standard deviation. The added term $\log(\text{GGALT})$ also provided some small additional improvement. To illustrate the result from this revised fit, measurements from flights 1, 2, 3, 6, 8, 9, 11, 14, and 18 were used to calculate the appropriate coefficients. These were chosen because these flights all individually provided reasonably consistent fit results, while excluded flights often did not. Some of the excluded flights were very short flights or were flights for diversion to other airports rather than for research. Figures 8 and 9 show that a significantly improved fit is obtained when dependence on QCF and $\log(\text{GGALT})$ is included, with the residual standard deviation reduced from 0.12 to 0.08° by inclusion of that dependence. The resulting vertical wind (Fig. 10) also shows important improvement over the vertical wind shown in Fig. 7, calculated

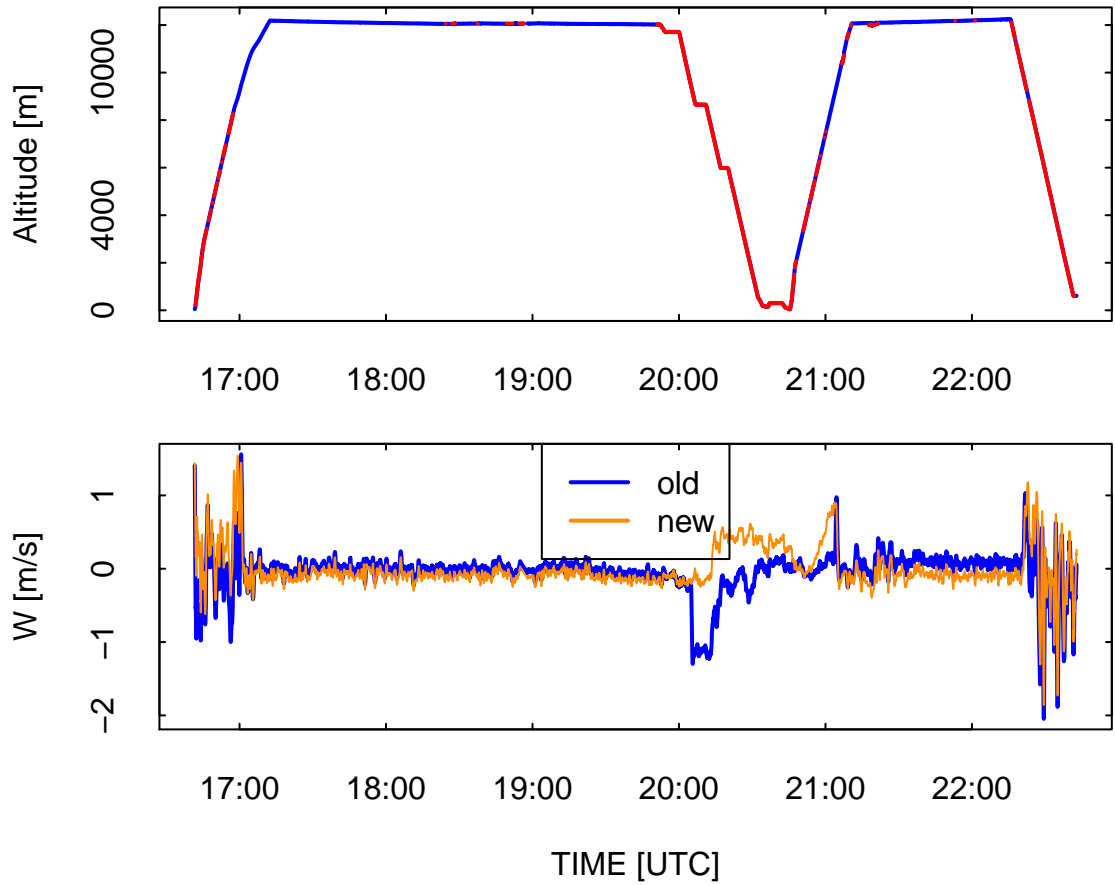


Figure 7: (top) Flight altitude during ORCAS flight 6, with blue lines indicating "normal" flight and red lines showing times when the aircraft configuration may not be normal. The bottom panel shows the corresponding new vertical wind calculated using the coefficients determined from this flight for the standard three-coefficient fit and repeats the values shown in Fig.3.

without inclusion of the additional factors. Inclusion of the variable K directly also provided significant improvement when tested alone, but not after inclusion of QCF, so K was not used, partly because uncertainty in weight of the aircraft, which enters K , appeared to lead to more variation from flight to flight. The single fit to the set of flights listed above provided a reasonably consistent representation of all ORCAS flights, as will be shown later. The following representation of angle of attack is a good candidate for representing vertical wind in ORCAS:

$$\alpha = a_0 + \frac{\text{ADIFR}}{\text{QCF}} (a_1 + a_2 M) + a_3 \text{QCF} + a_4 \ln(\text{GGALT}) \quad (6)$$

where the coefficients $\{a_0 - a_4\}$ are $\{4.555, 17.185, 2.544, -0.004, 0.01\}$.

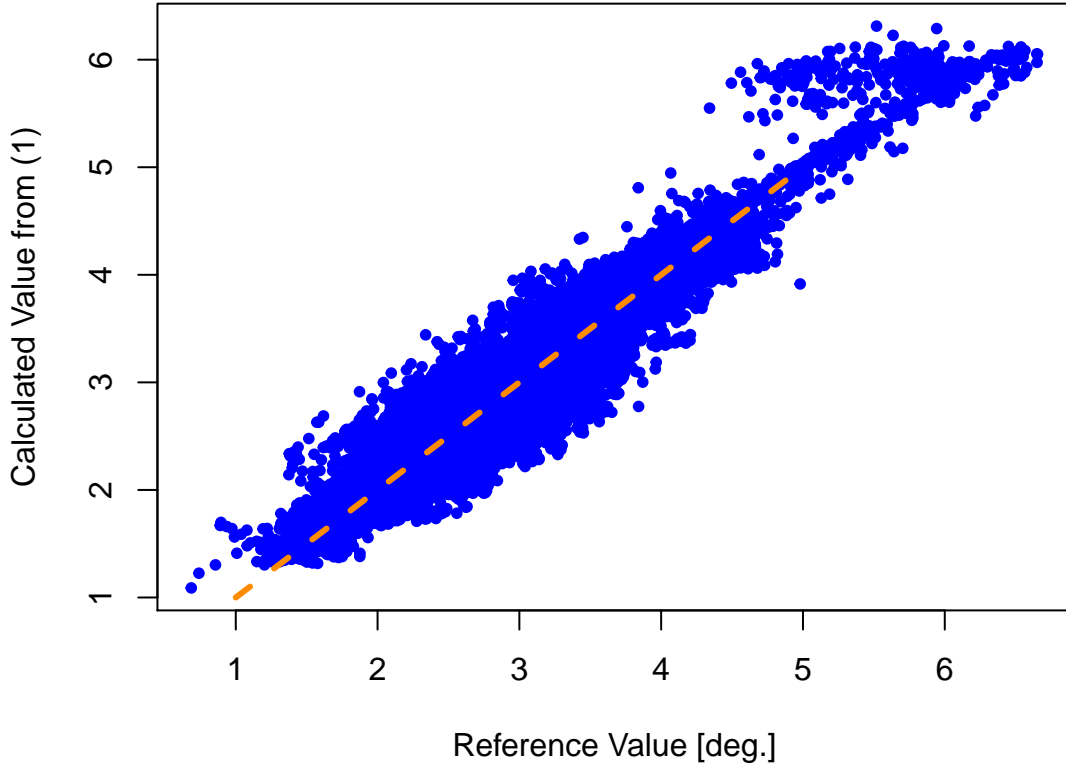


Figure 8: Revised fit using data from ORCAS flights 1, 2, 3, 6, 8, 9, 11, 14, 18, qualified as described in the text. This fit includes dependence on QCF, and $\log(\text{GGALT})$.

4.3 Fitting high-frequency and low-frequency components separately

Still another approach is tried next. It is based on representing the high-frequency and low-frequency contributions to angle of attack separately. The reason for this approach is that the fluctuations and the offset in angle of attack seem to require different representations, so a single representation like that in (1) or (6) has difficulty matching both the amplitude of fluctuations and the variation of the mean during the flight. Separating the contributions into two components and fitting them separately might provide a better representation of the angle of attack.

The steps are these:

1. Separate α^* into two components using a low-pass filter for the slowly varying component and the complementary high-pass filter for the fast-varying component, so that $\alpha^* = \alpha_f^* + \alpha_s^*$. Here a cutoff frequency corresponding to a period of 600 s will be used.. Also calculated

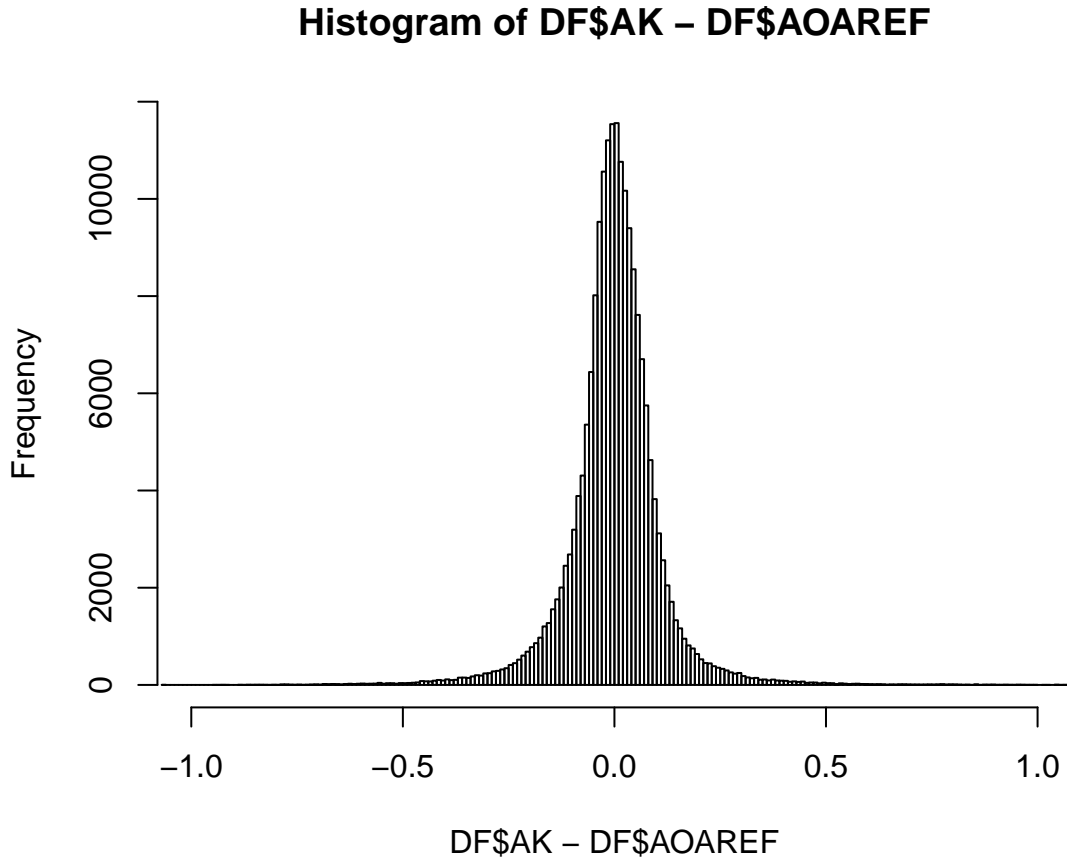


Figure 9: Histogram of the difference between the two estimates of angle of attack, as represented by the fit and as represented by the reference value.

similar low-pass-filtered and high-pass-filtered values for the variables $A = \Delta p_\alpha/q$ (AD-IFR/QCF) and M (Mach number), and also q (QCF) for possible use in fitting..

2. For the high-frequency component, find a representation having the simple form

$$\alpha_f^* = c_0 + c_1 A_f \quad (7)$$

For this fit, restrict the measurements to be fit to $TASX > 110$ and $|ROLL| < 2$, and to avoid end effects of the filter exclude about 1.5 times the filter time constant from the start and end of the time series. (This functional form was found to be adequate and additional terms are not needed.)

3. For the low-frequency component, use a more complicated 5-coefficient fit, which leads to a significant improvement over the two-coefficient fit:

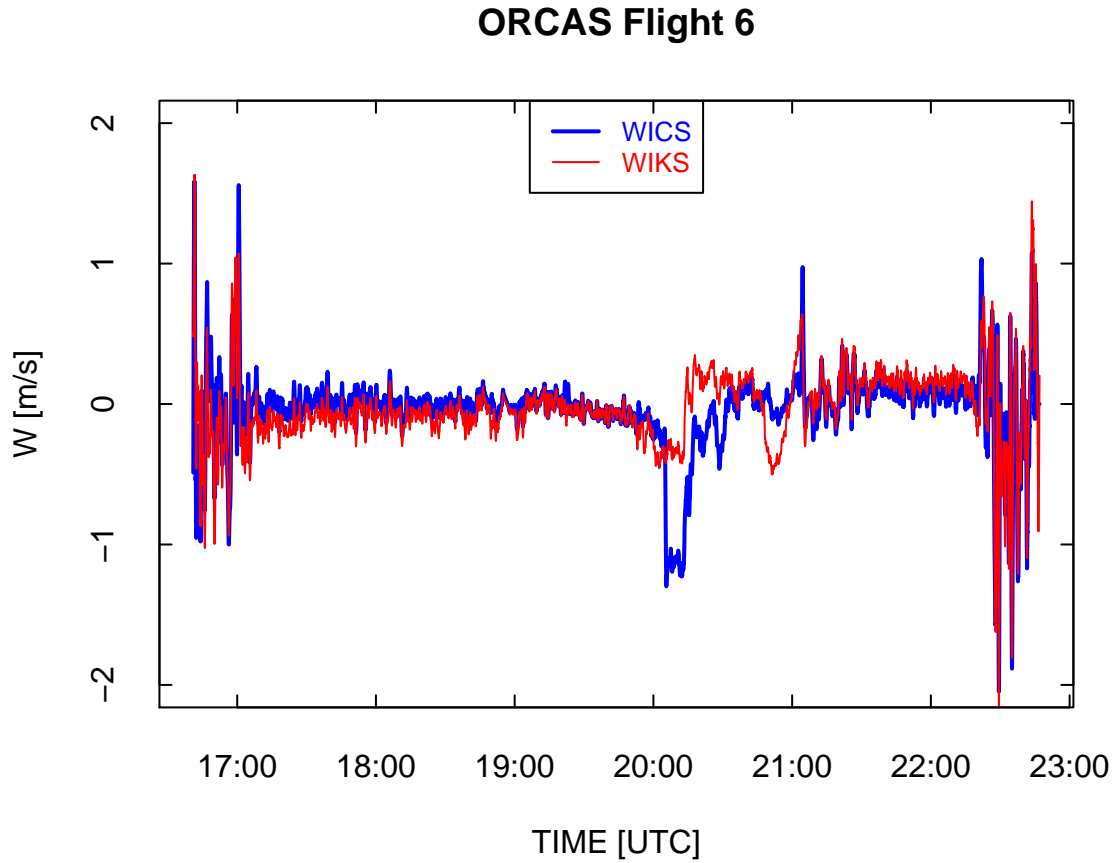


Figure 10: Vertical wind for ORCAS flight 6, calculated using the angle-of-attack calculated as in the preceding two figures where QCF and log(GGALT) were added terms in the fit.

$$\alpha_s^* = d_0 + d_1 A_s + d_2 (A_s M_s) + d_3 M_s + d_4 q_s \quad (8)$$

Then find the resulting parameterized representation of the angle of attack from the sum of these equations:

$$\alpha = c_0 + c_1 A_f + d_0 + d_1 A_s + d_2 A_s M_s + d_3 M_s + d_4 q_s = \alpha_f + \alpha_s \quad (9)$$

```
## lm(formula = AOAREFF ~ QRF, data = DF)
## [1] "Coefficients:"
##                               Estimate Std. Error t value Pr(>|t|)
## (Intercept)  0.00314   0.000216   14.5 1.09e-47
## QRF        18.38628   0.029259   628.4 0.00e+00
```

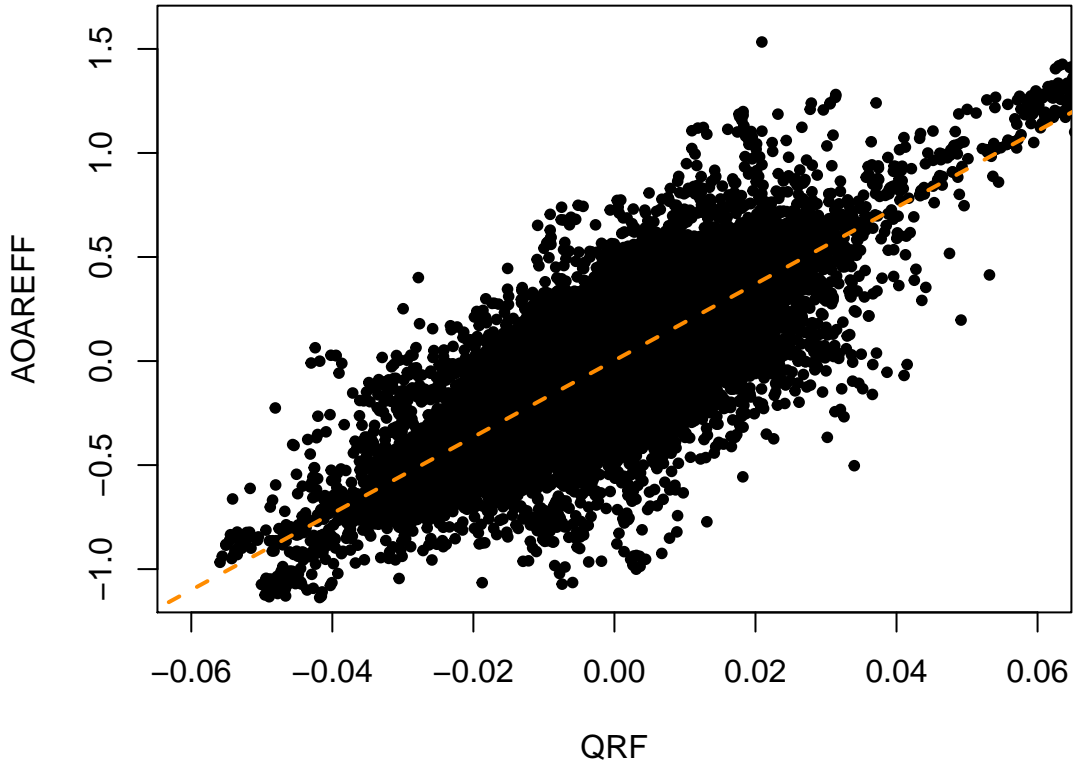


Figure 11: The high-pass value of the reference angle α_f^* plotted vs. the high-pass version of the ratio of ADIFR to QCF, for ORCAS flight 6.

```
## [1] "Residual standard deviation: 0.093, dof=185301"  
## [1] "R-squared 0.681"
```

```
## lm(formula = AOAREFS ~ QRS + I(QRS * MS) + MS + QCFS, data = DF)  
## [1] "Coefficients:"  
##             Estimate Std. Error t value Pr(>|t|)  
## (Intercept) 4.37242  1.70e-03   2571      0  
## QRS         14.61443  2.03e-02    718      0  
## I(QRS * MS) 7.38942  3.13e-02    236      0  
## MS          0.43072  2.19e-03    196      0  
## QCFS        -0.00344  8.75e-06   -393      0  
## [1] "Residual standard deviation: 0.039, dof=186209"
```

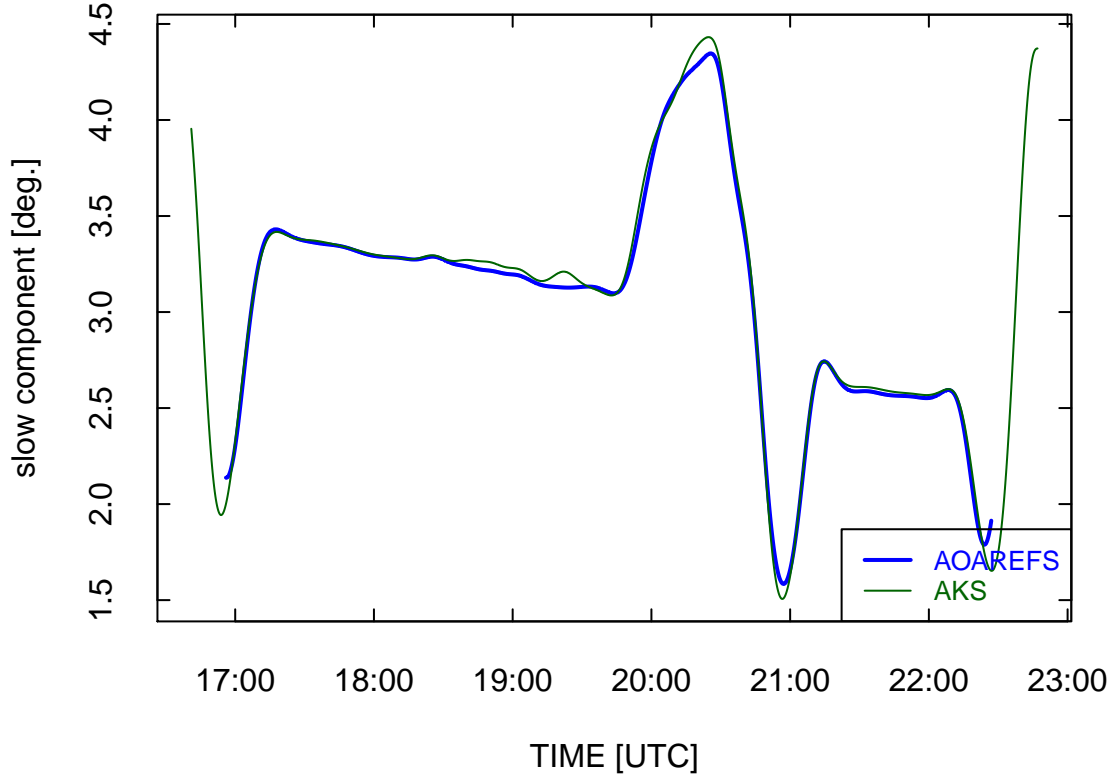


Figure 12: The low-pass component of the reference AOAREFS and the result from the fit to this component for the five-coefficient fit, for ORCAS flight 6.

```
## [1] "R-squared 0.993"
```

The same set of flights as used in the preceding subsection were used for this fit. The result for the high-frequency fit is $\{c_0, c_1\} = \{0.003, 18.386\}$, and the result for the low-pass-filtered component is $\{d_0, d_1, d_2, d_3\} = \{4.372, 14.614, 7.389, 0.431\}$. The coefficient c_0 is near zero as expected and should be omitted. For the composite data set, both gave good fits, with residual standard deviations of 0.093 and 0.039 respectively for the high-frequency and low-frequency components. The latter is a very good representation of the slowly varying component, while the former will be affected by real fluctuations in the vertical wind and so is expected to be larger. Figure 11 shows that the resulting high-frequency component matches the reference value very well, while Fig. 12 shows similar good agreement for the slowly varying component. The vertical wind, shown in Fig. 13 for ORCAS flight 6, also appears very good. The deviation in vertical wind near 21:05:00 UTC appears consistent with a real fluctuation, although it is also near where the aircraft passes

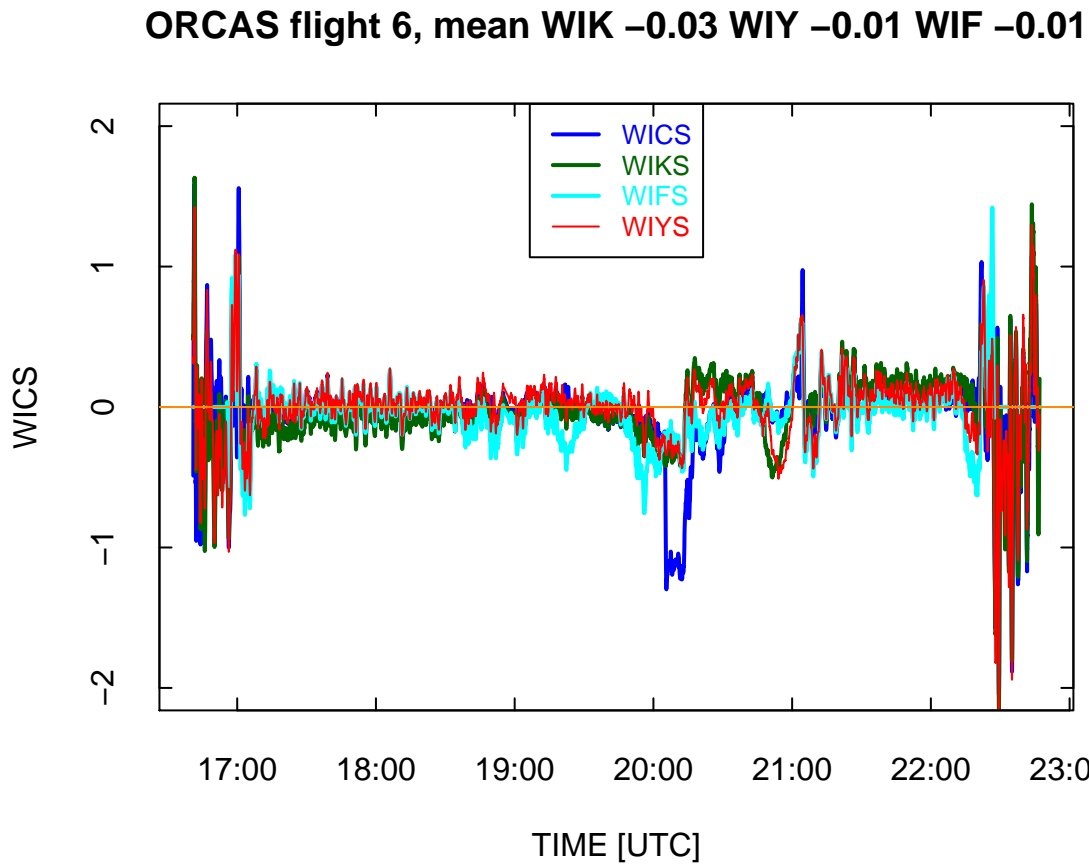


Figure 13: The vertical wind obtained by calculating the two filtered components separately and adding them to obtain the angle of attack (red line). Also shown is the fit result obtained using the five-coefficient fit from the previous section (green line) and the result of filtering WIK (cyan line).

through 25,000 ft and this often seems to correlate with a perturbation in vertical wind. (It is also, perhaps coincidentally, the altitude limit for the use of any flaps.) Other small perturbations near 20:00:00 are more suspicious and may be remnant effects of the aerodynamic effects discussed in the previous section.

The four vertical wind candidates, shown for each flight in plots appended to this report, are:

1. (blue) WICS: The original vertical wind in the EOL files.
2. (green) WIKS: The vertical wind determined by fits that include two additional terms, using data for flights 1, 2, 3, 6, 8, 9, 11, 14, and 18 to determine one 5-coefficient all-project fit and then applying that result to all flights. The added terms in the fit are QCF and log(GGALT).
3. (red) WIYS: The vertical wind determined by separating angle-of-attack into two compo-

nents by complementary filtering and then fitting the two components separately, before adding the result. This differs from the next component, WIFS, in representing the low-frequency component by a fit to the calibration data (that assumes vertical wind of zero) rather than eliminating it as in WIFS.

4. (cyan) WIFS: The filtered vertical wind determined from the high-frequency component in WIYS, with the low-frequency component represented by the low-pass filtered version of the reference angle-of-attack. In this case, real fluctuations with duration longer than the cut-off period (here, 600 s) are removed, while they are retained in WIYS.

5 Recommendation

The variable WIY appears to be the best representation of vertical wind, but there is little difference between WIY and WIK so WIY might support the use of WIK. The disadvantage of WIY is that it requires post-processing because it involves filtering to determine the two components that enter the result, application of empirical coefficients separately to the two components, and summing the results. The result, however, is not a filtered result, and it will not distort from real offsets in the vertical wind except as they affect the estimation of the empirical coefficients. This variable then appears better than straight high-pass filtering of the vertical wind. A post-processing step similar to that used in HIPPO-5 could be developed to implement this scheme, and appropriate coefficients are listed in Sect. 4.3. The variable WIK, however, is almost as good and has the significant advantage that it would be incorporated into the first-pass processing. The appropriate formula and coefficients are listed at the end of Sect. 4.2.

Memo to: ORCAS data-processing file

1 November 2016

Page 18

– End of Memo –

Reproducibility:

PROJECT: AKRDforORCAS
ARCHIVE PACKAGE: AKRDforORCAS.zip
CONTAINS: attachment list below
PROGRAM: AKRDforORCAS.Rnw
THIS DOCUMENT: AKRDforORCAS.pdf
WORKFLOW: WorkflowAKRDforORCAS.pdf
ORIGINAL DATA: /scr/raf_data/ORCAS/ORCASrf01.nc, etc
DATA ARCHIVE: NCAR HPSS (not github) AKRDforORCAS.Rdata
GIT: <https://github.com/WilliamCooper/Reprocessing.git> – see above files

Attachments: AKRDforORCAS.Rnw
AKRDforORCAS.pdf
WorkflowAKRDforORCAS.pdf
SessionInfo

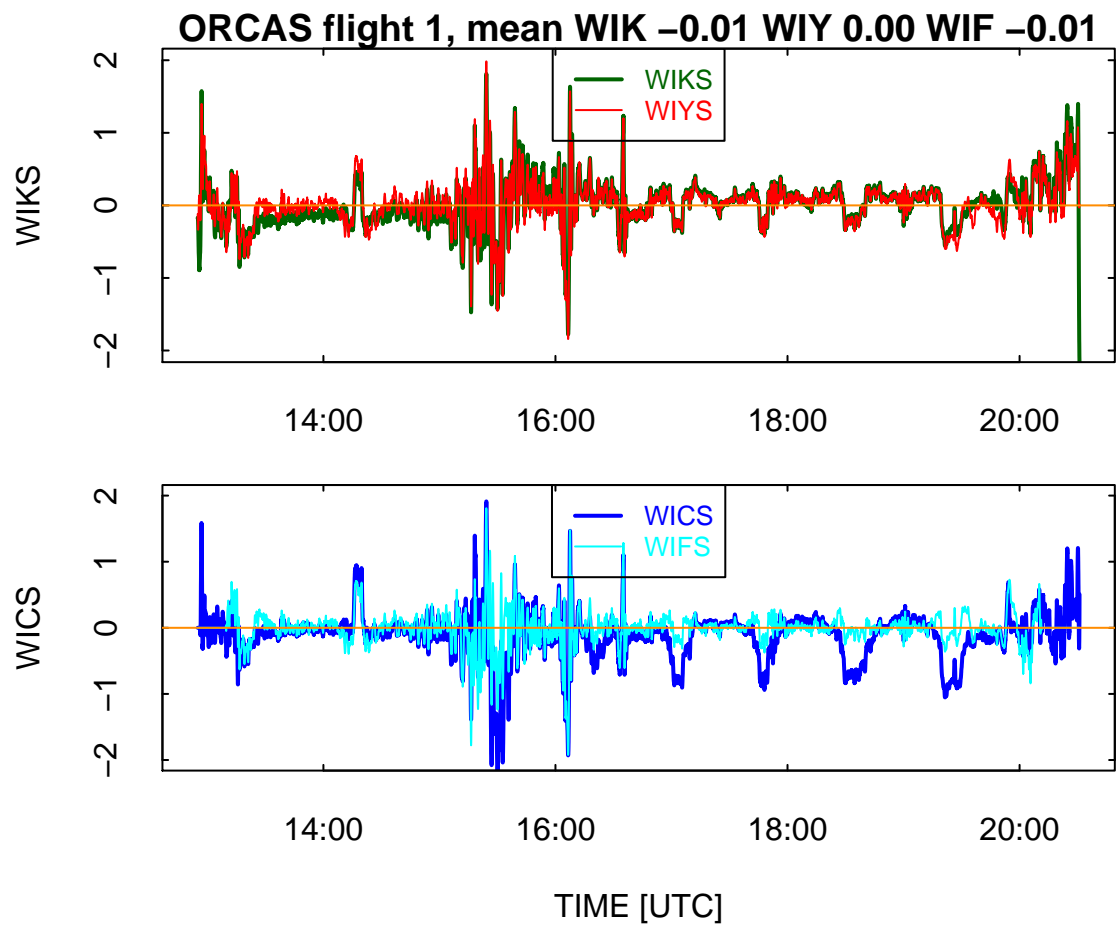


Figure 14: Plots for each ORCAS flight showing the four candidates for vertical wind.

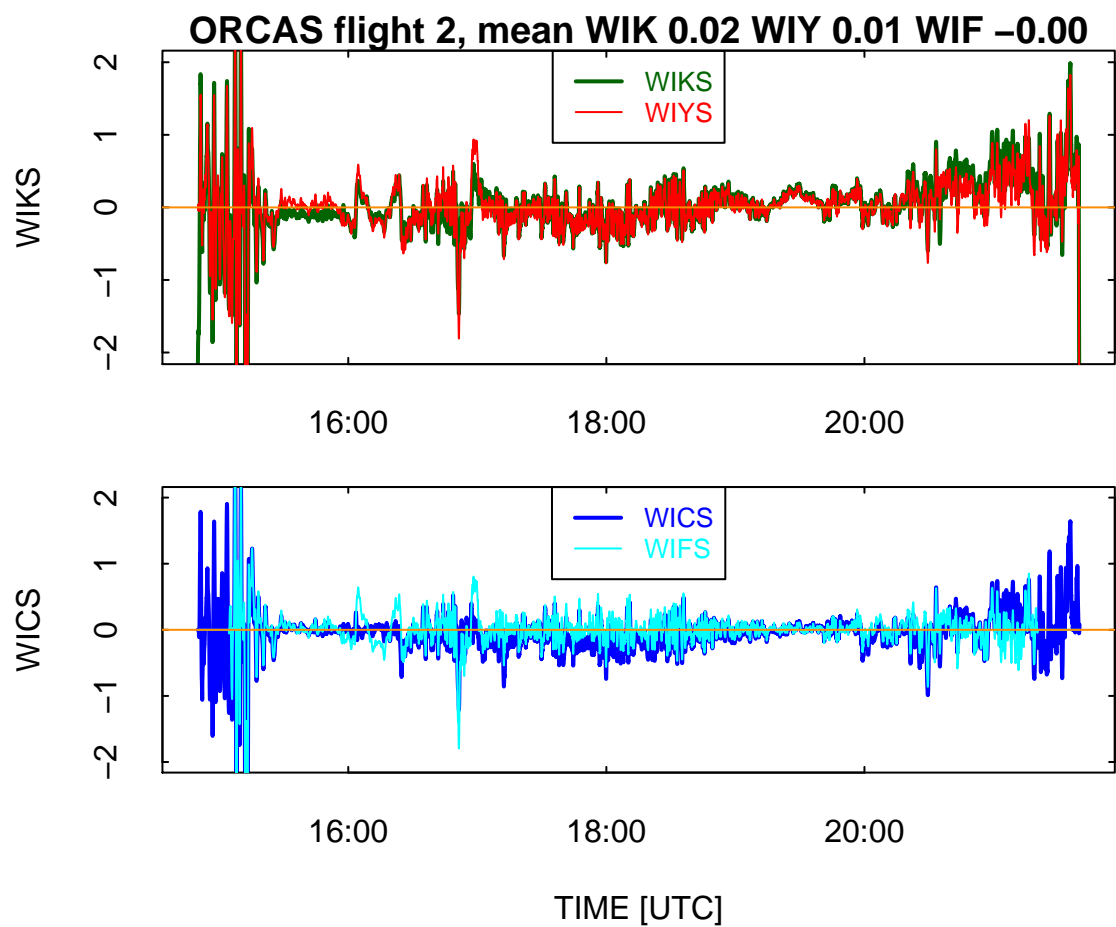


Figure 15: Plots for each ORCAS flight showing the four candidates for vertical wind.

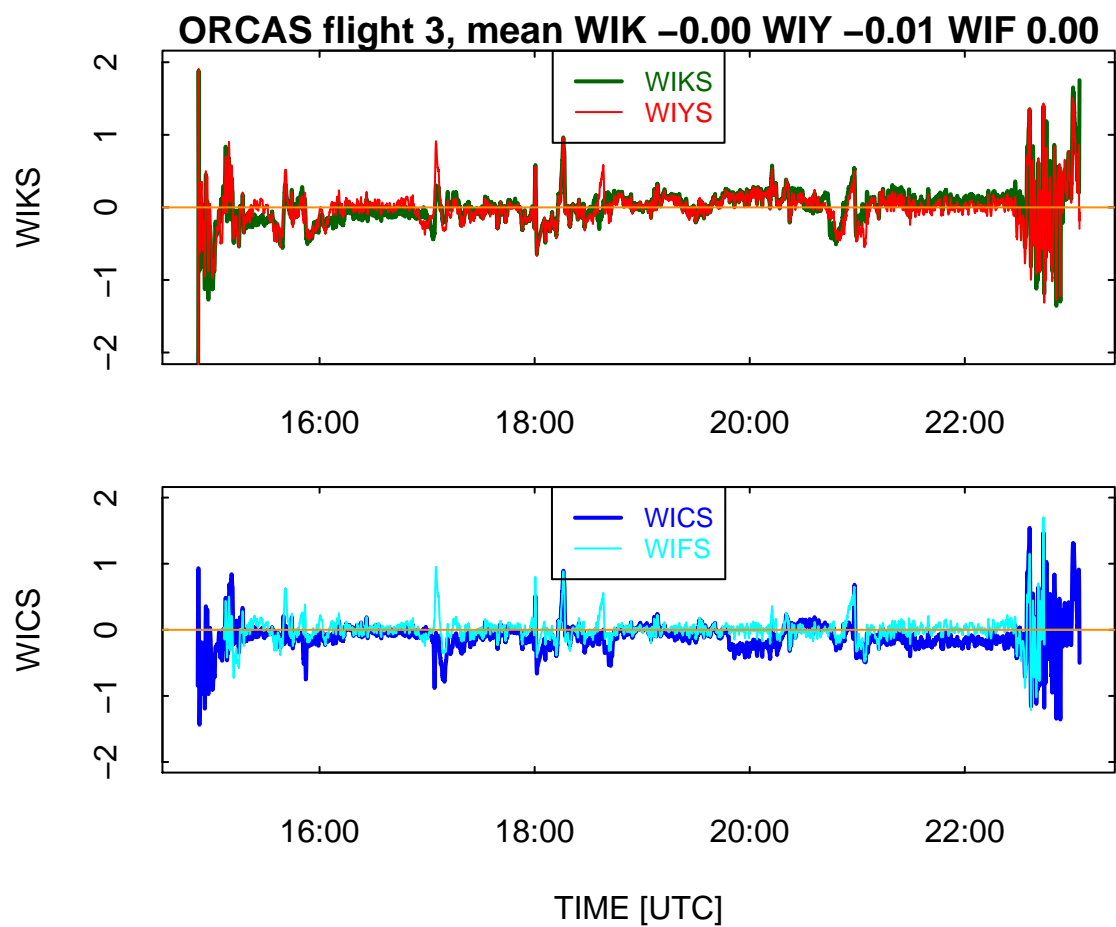


Figure 16: Plots for each ORCAS flight showing the four candidates for vertical wind.

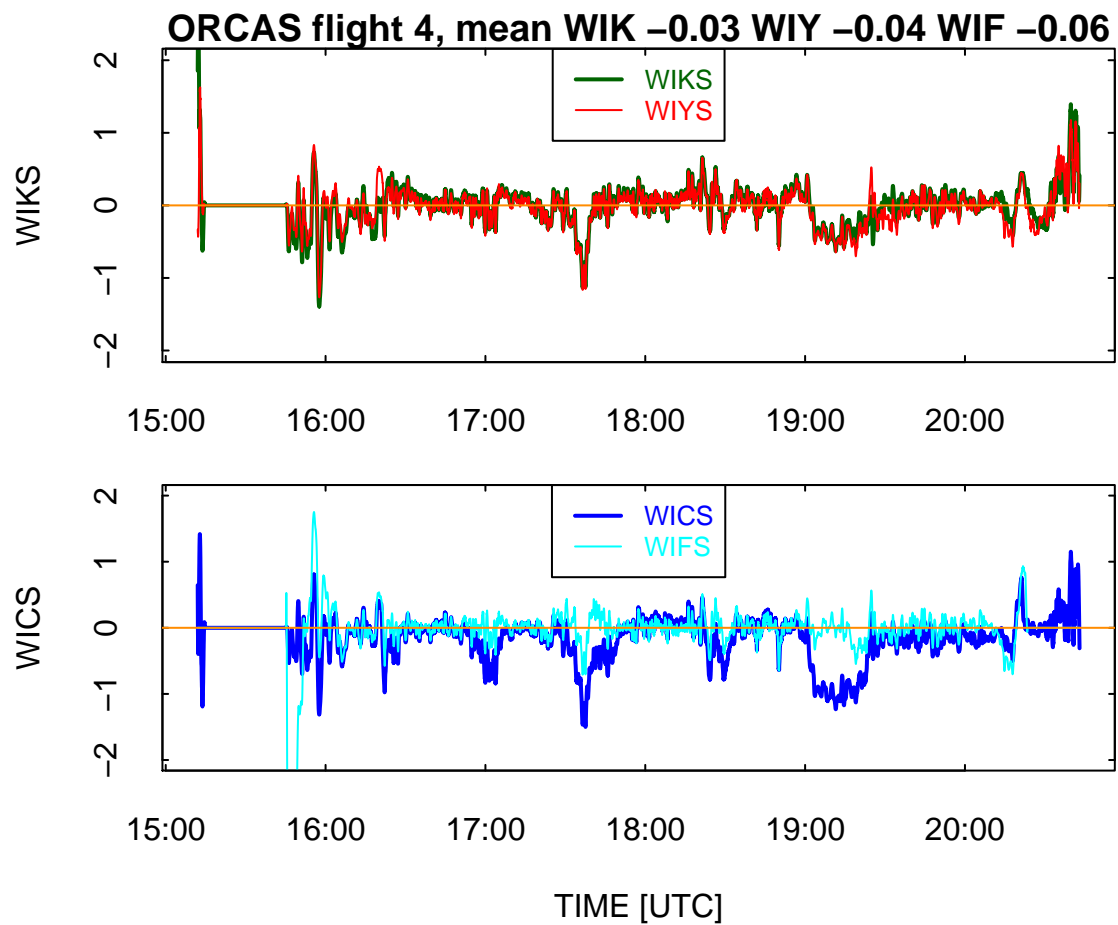


Figure 17: Plots for each ORCAS flight showing the four candidates for vertical wind.

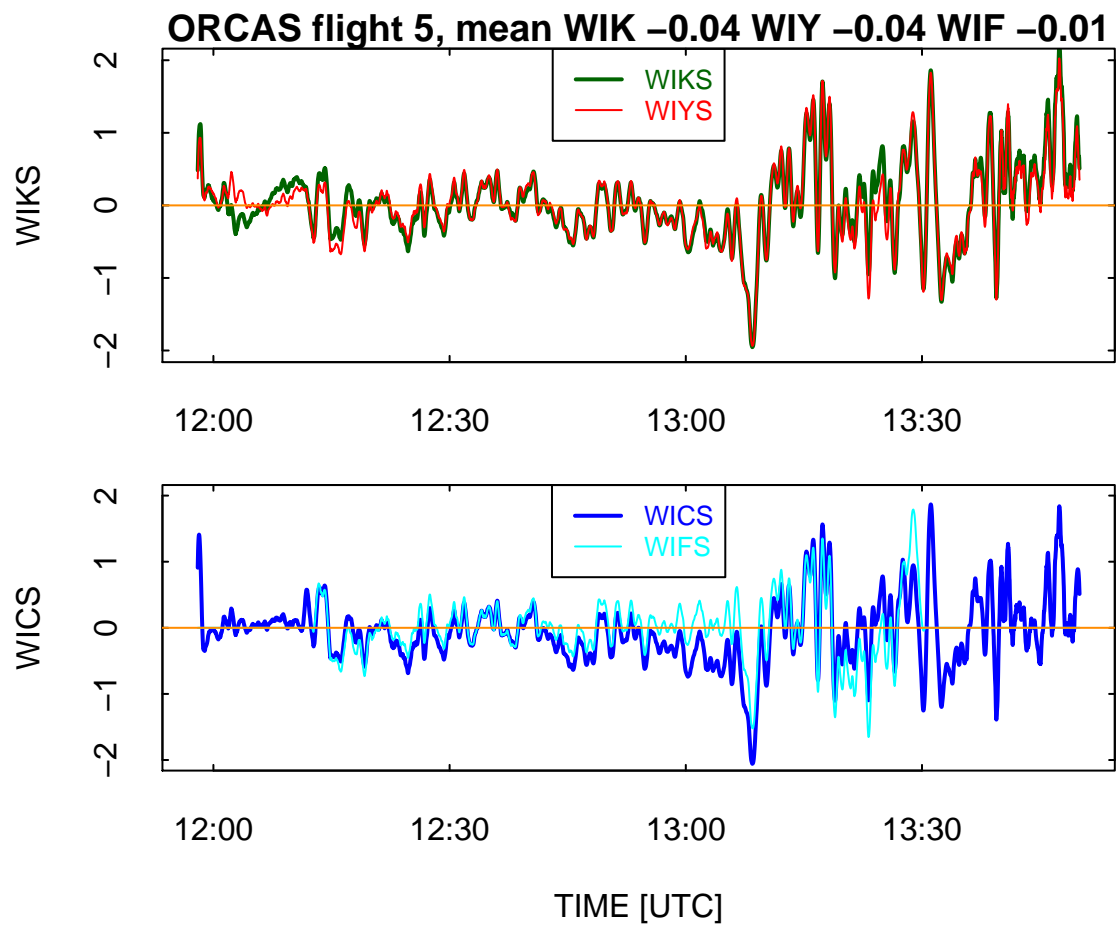


Figure 18: Plots for each ORCAS flight showing the four candidates for vertical wind.

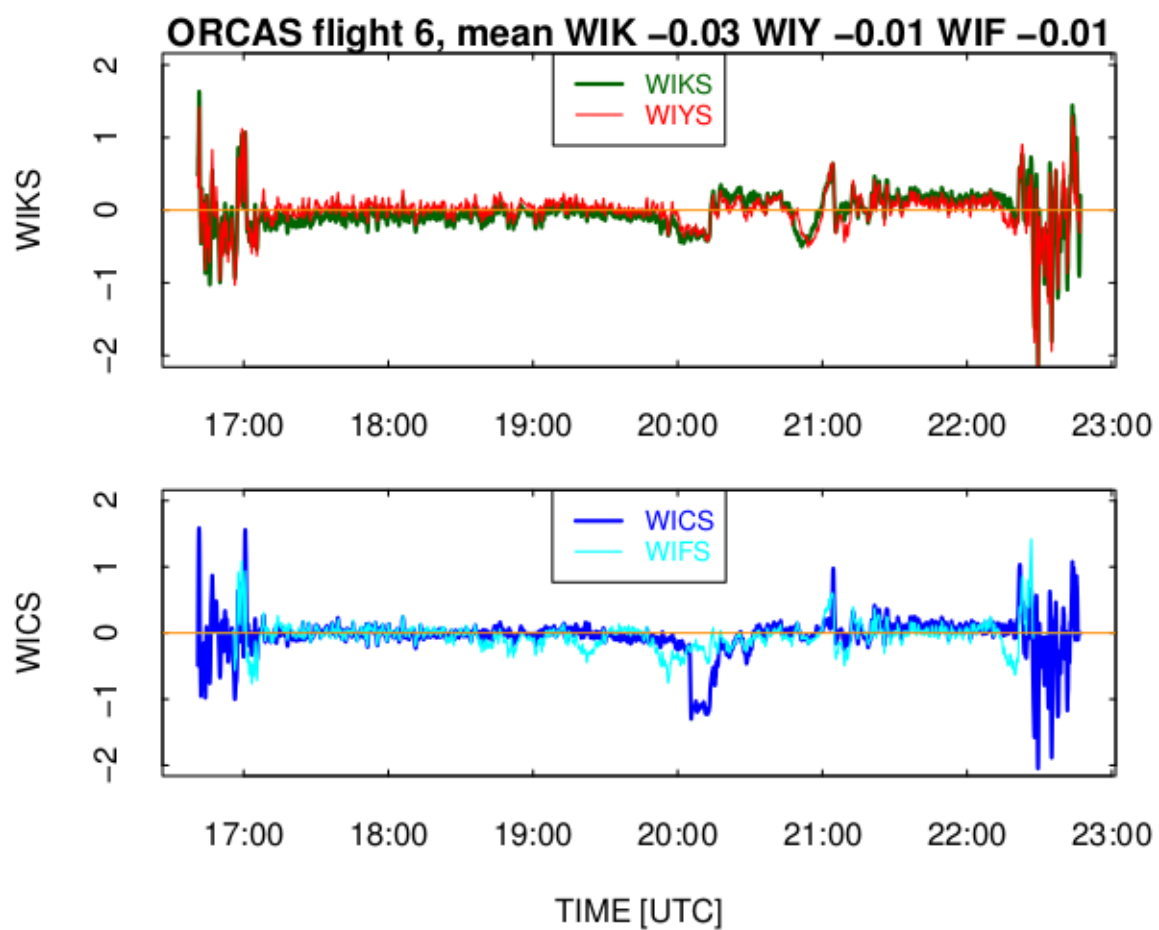


Figure 19: Plots for each ORCAS flight showing the four candidates for vertical wind.

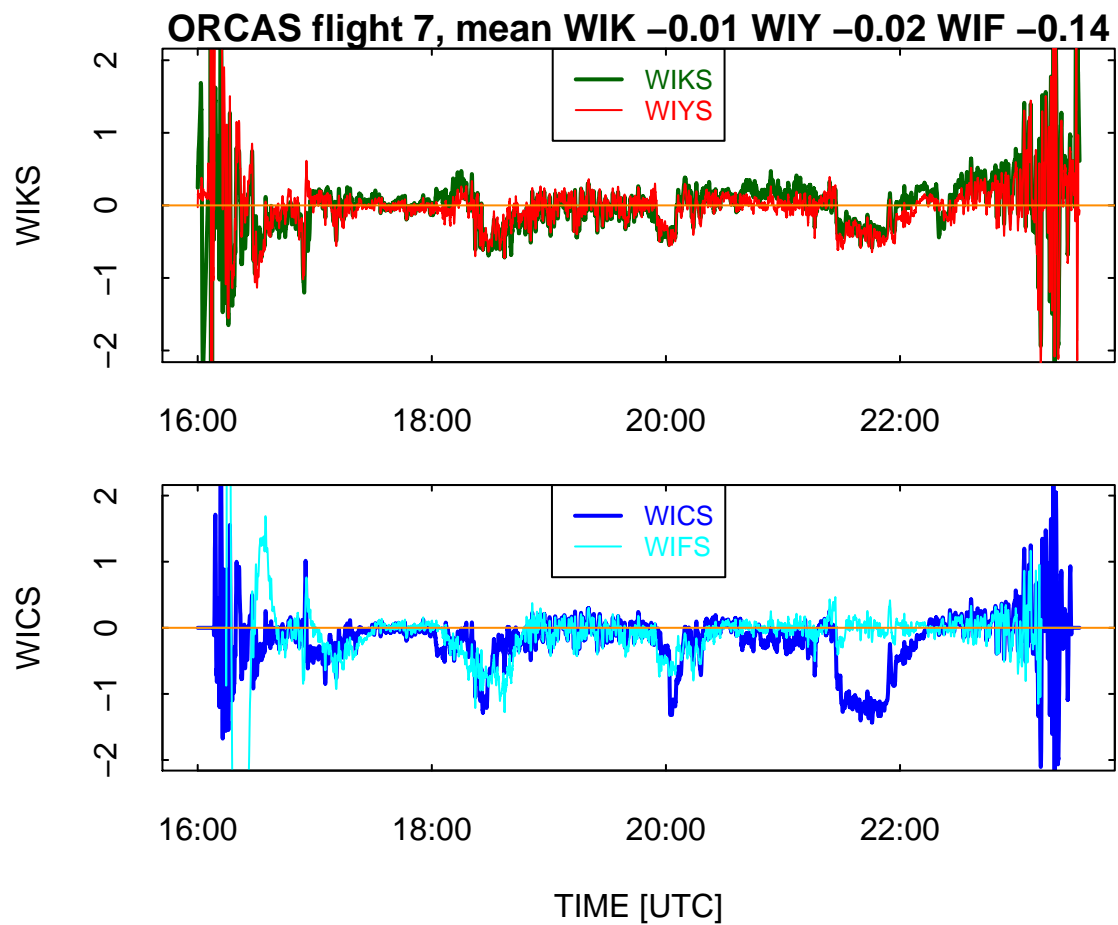


Figure 20: Plots for each ORCAS flight showing the four candidates for vertical wind.

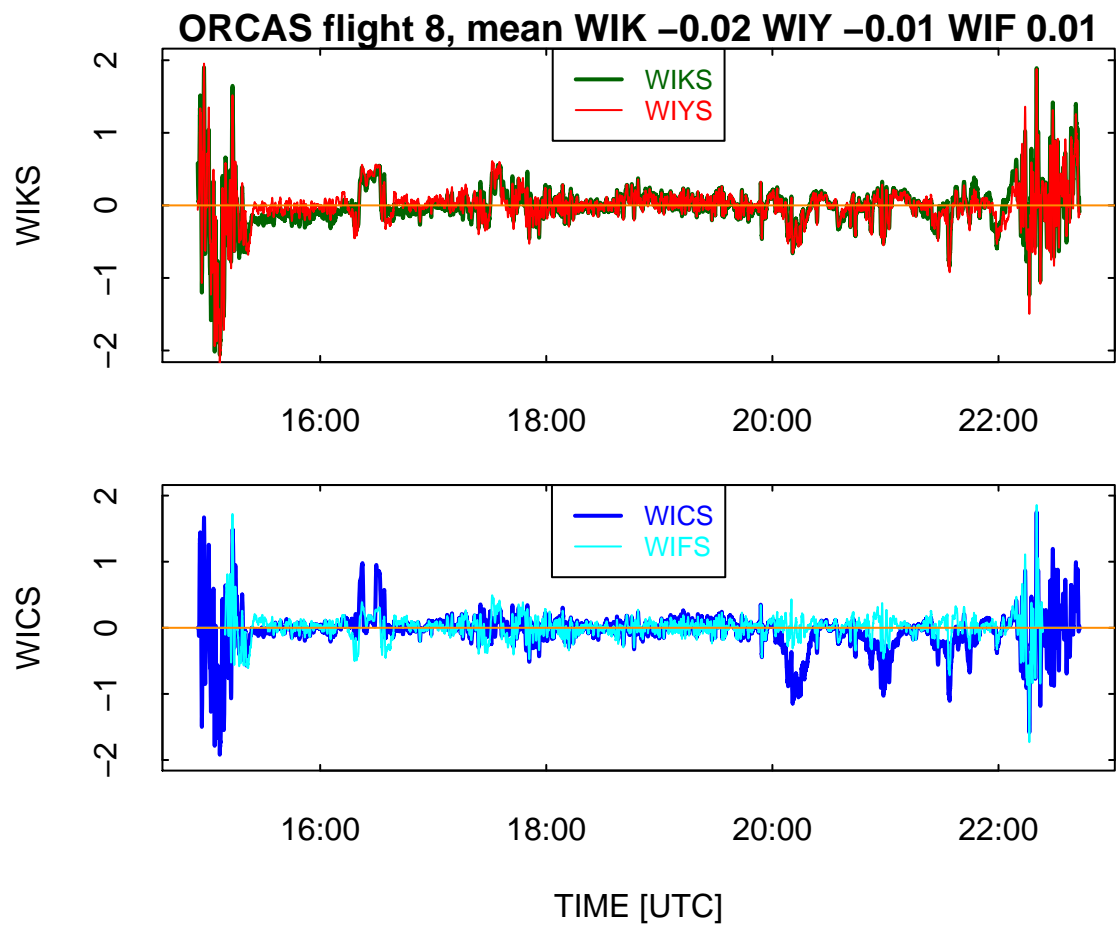


Figure 21: Plots for each ORCAS flight showing the four candidates for vertical wind.

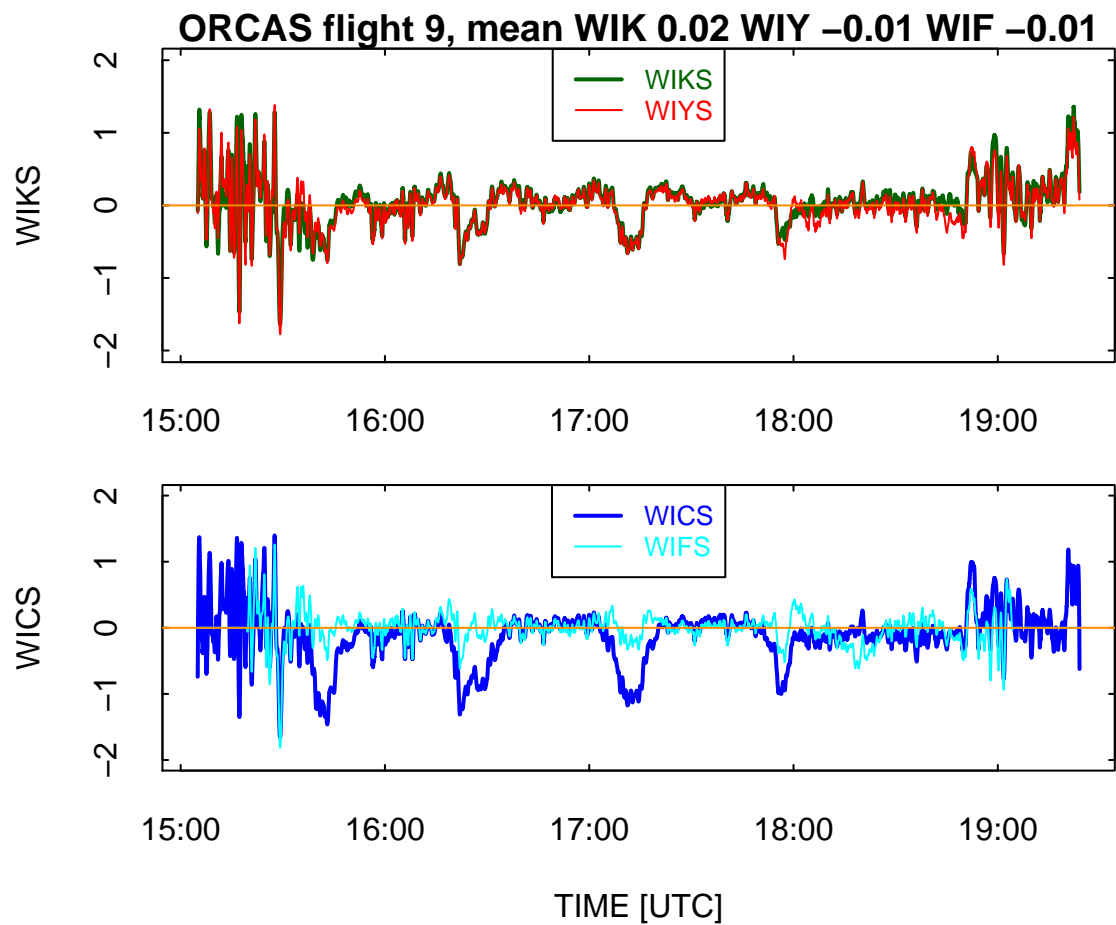


Figure 22: Plots for each ORCAS flight showing the four candidates for vertical wind.

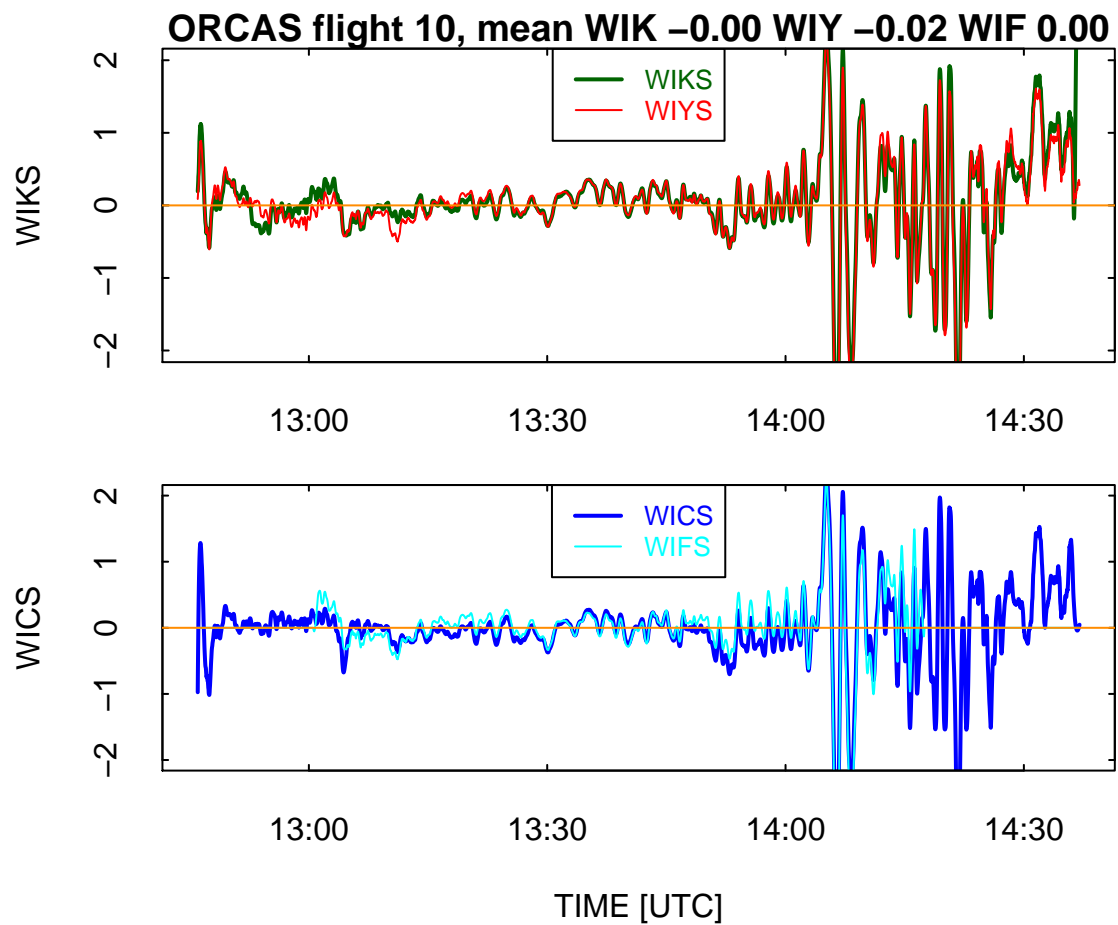


Figure 23: Plots for each ORCAS flight showing the four candidates for vertical wind.

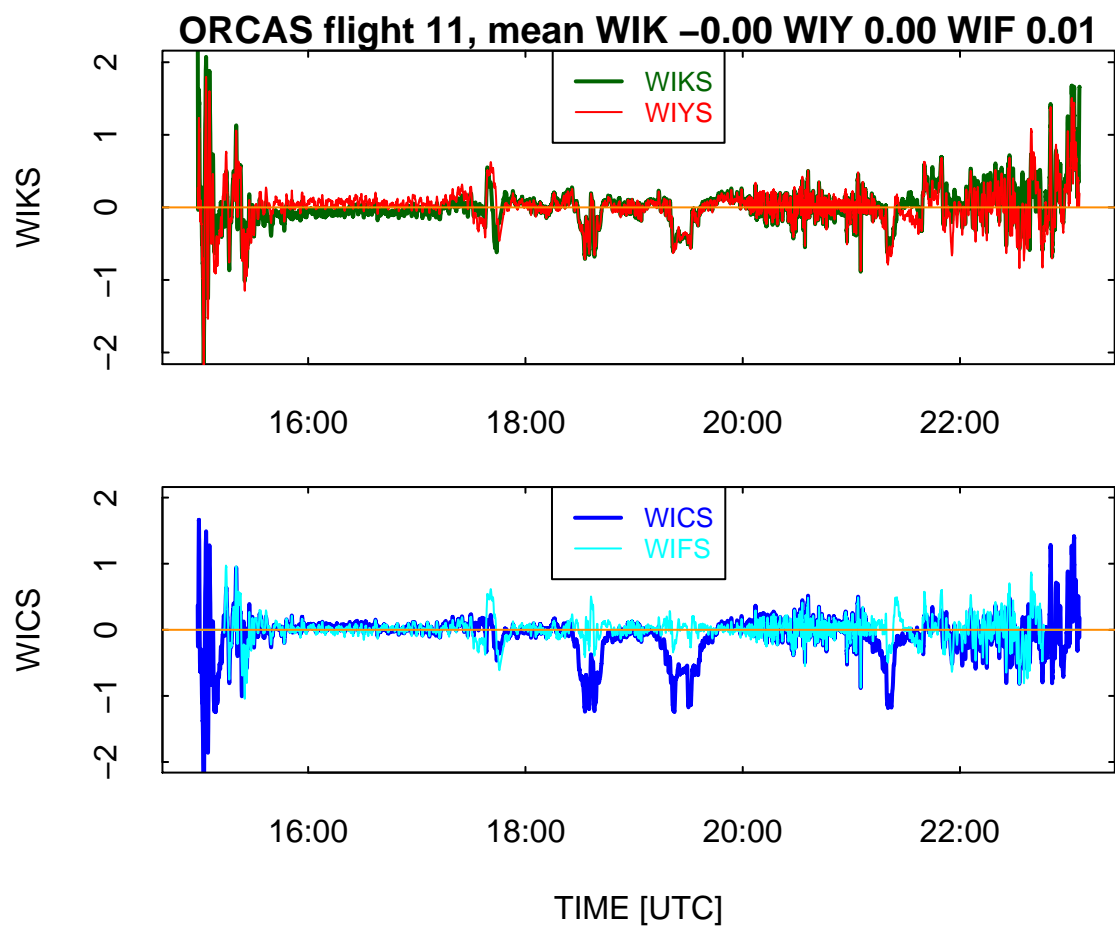


Figure 24: Plots for each ORCAS flight showing the four candidates for vertical wind.

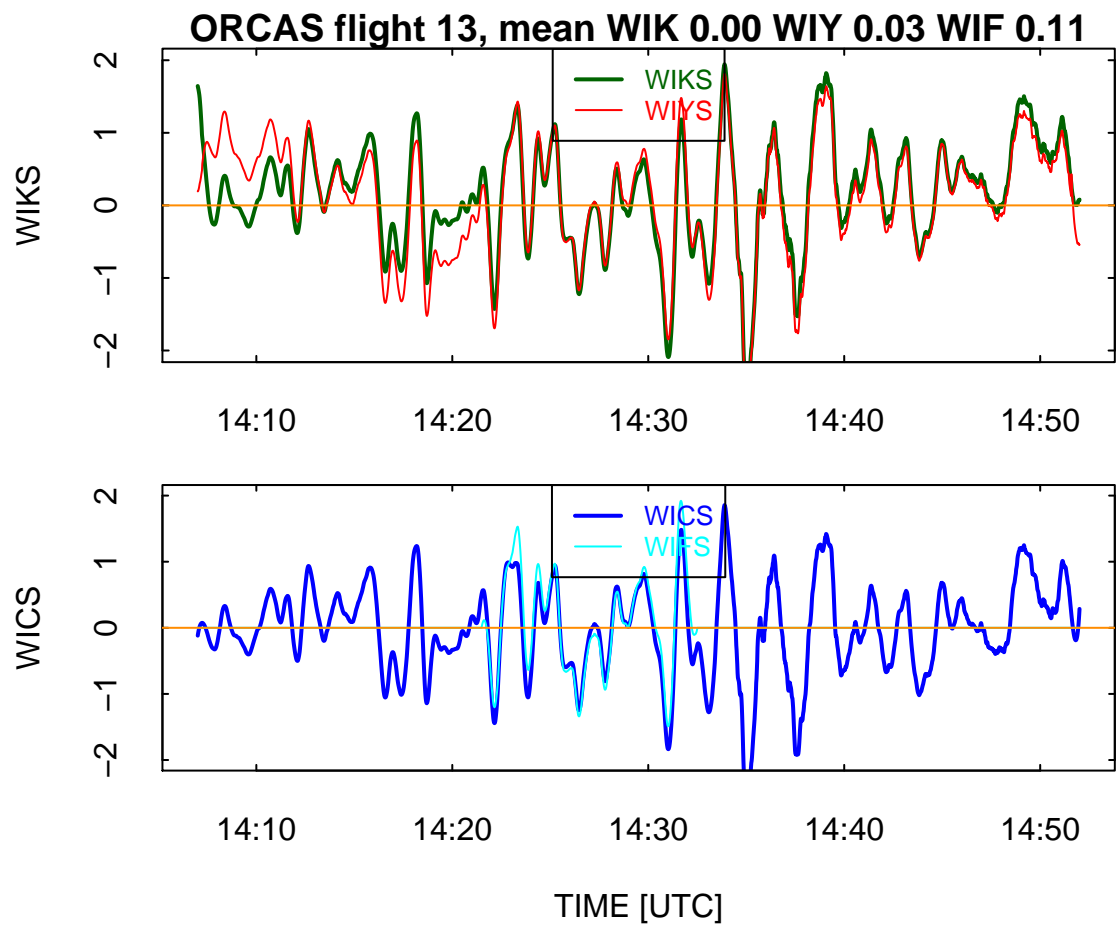


Figure 25: Plots for each ORCAS flight showing the four candidates for vertical wind.

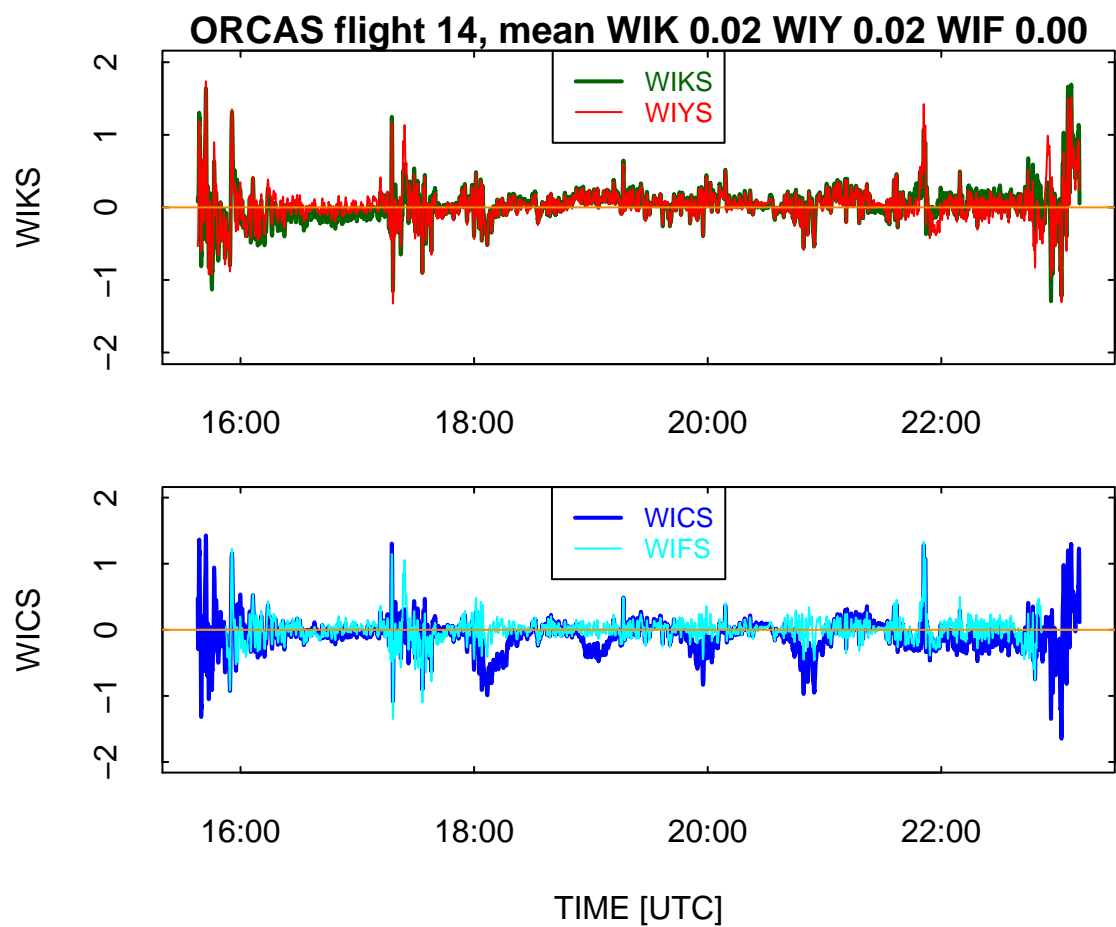


Figure 26: Plots for each ORCAS flight showing the four candidates for vertical wind.

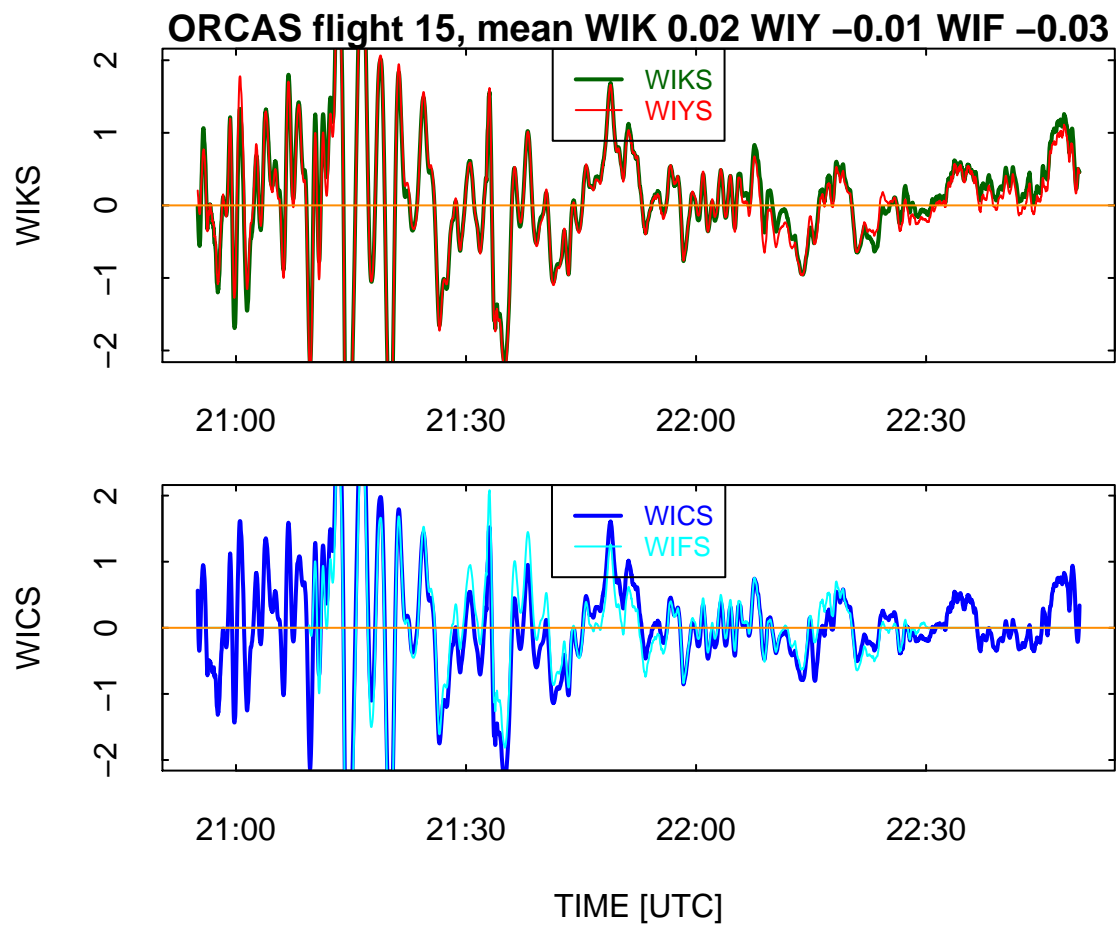


Figure 27: Plots for each ORCAS flight showing the four candidates for vertical wind.

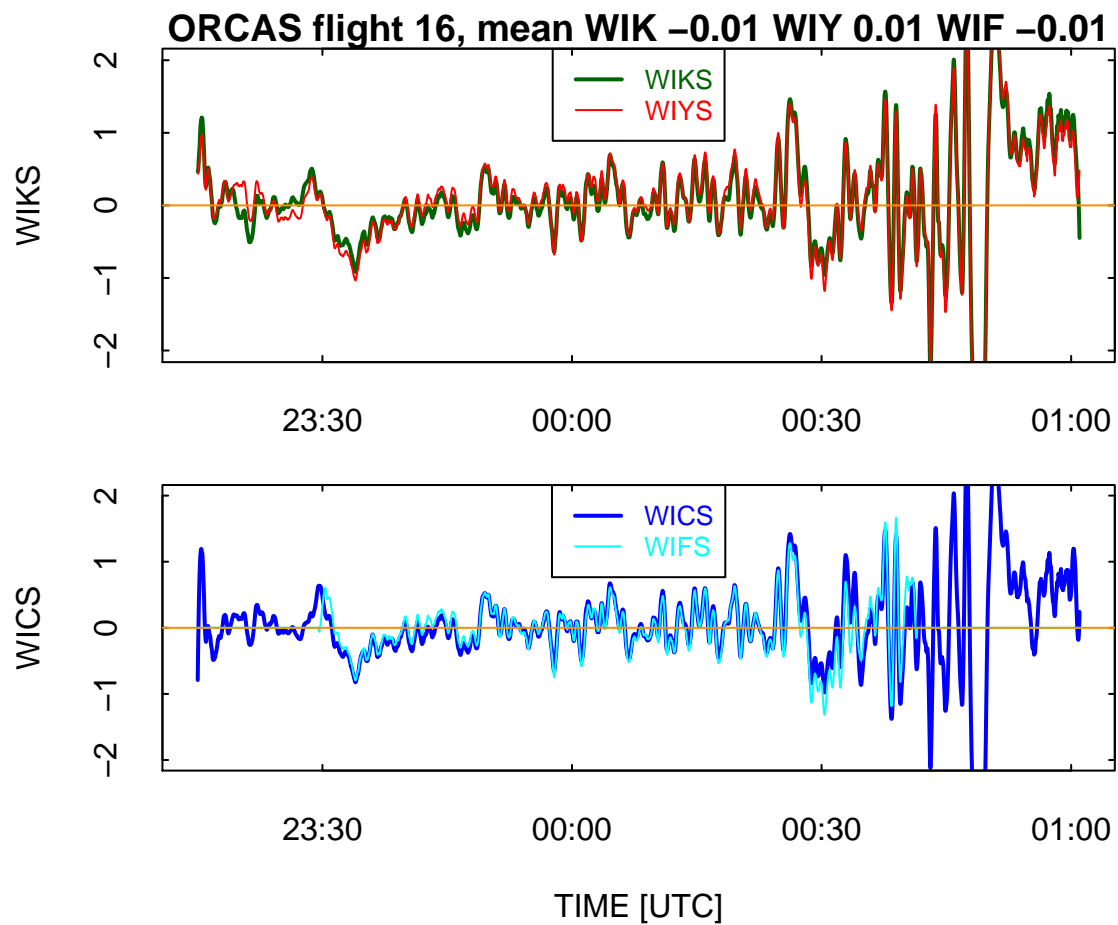


Figure 28: Plots for each ORCAS flight showing the four candidates for vertical wind.

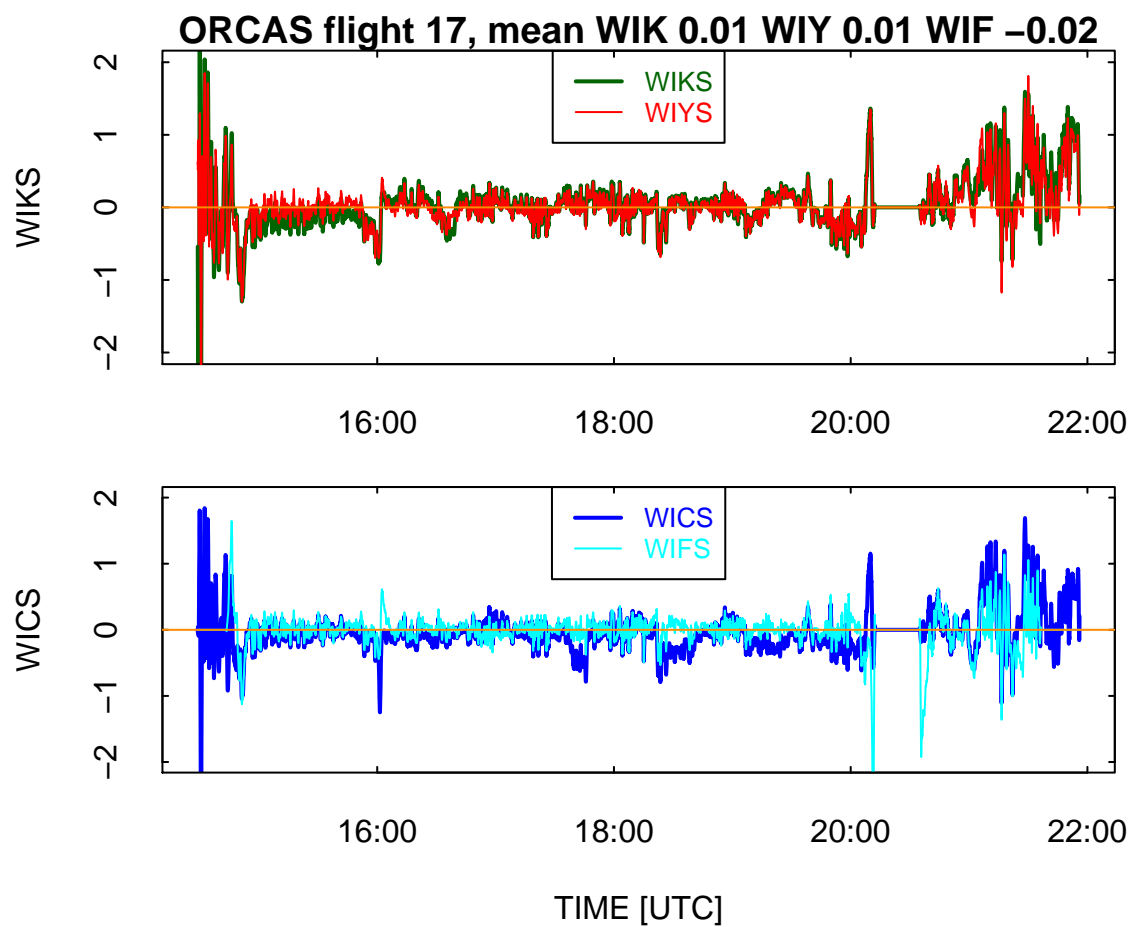


Figure 29: Plots for each ORCAS flight showing the four candidates for vertical wind.

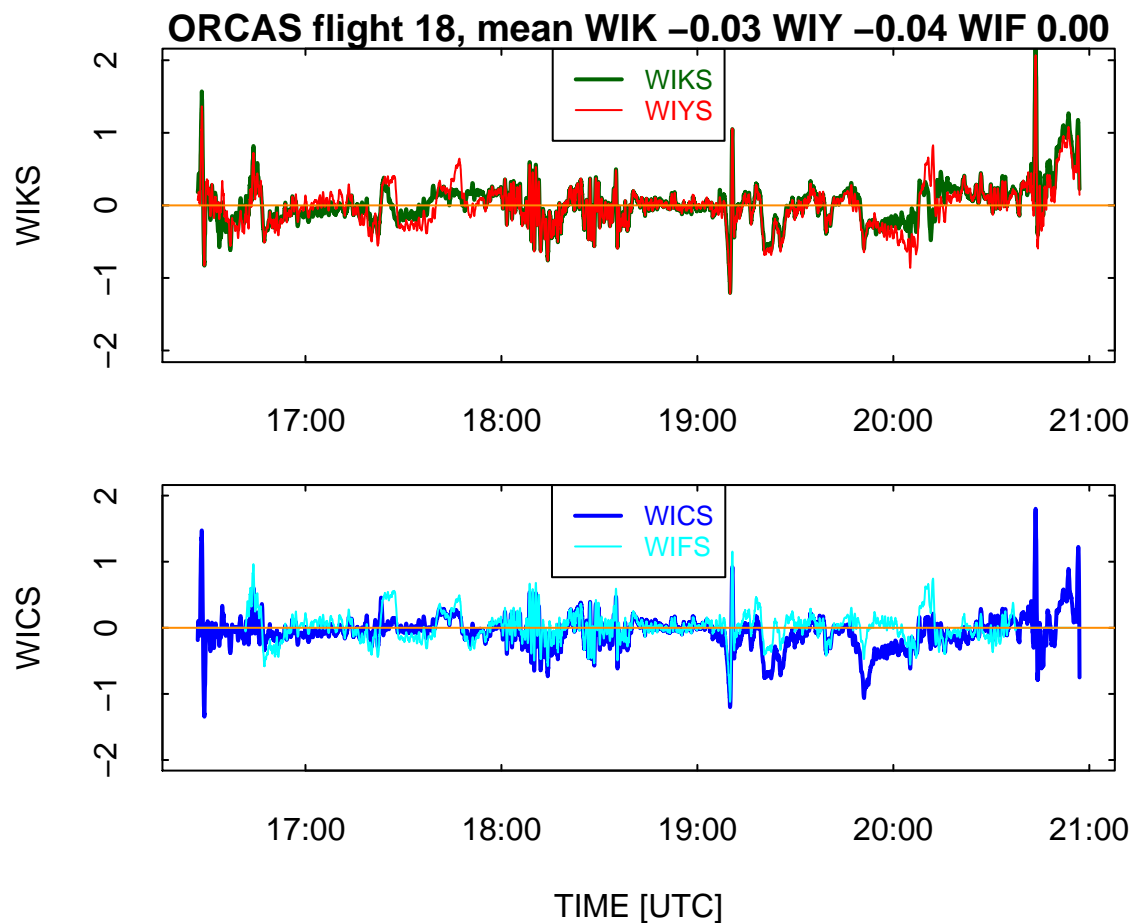


Figure 30: Plots for each ORCAS flight showing the four candidates for vertical wind.

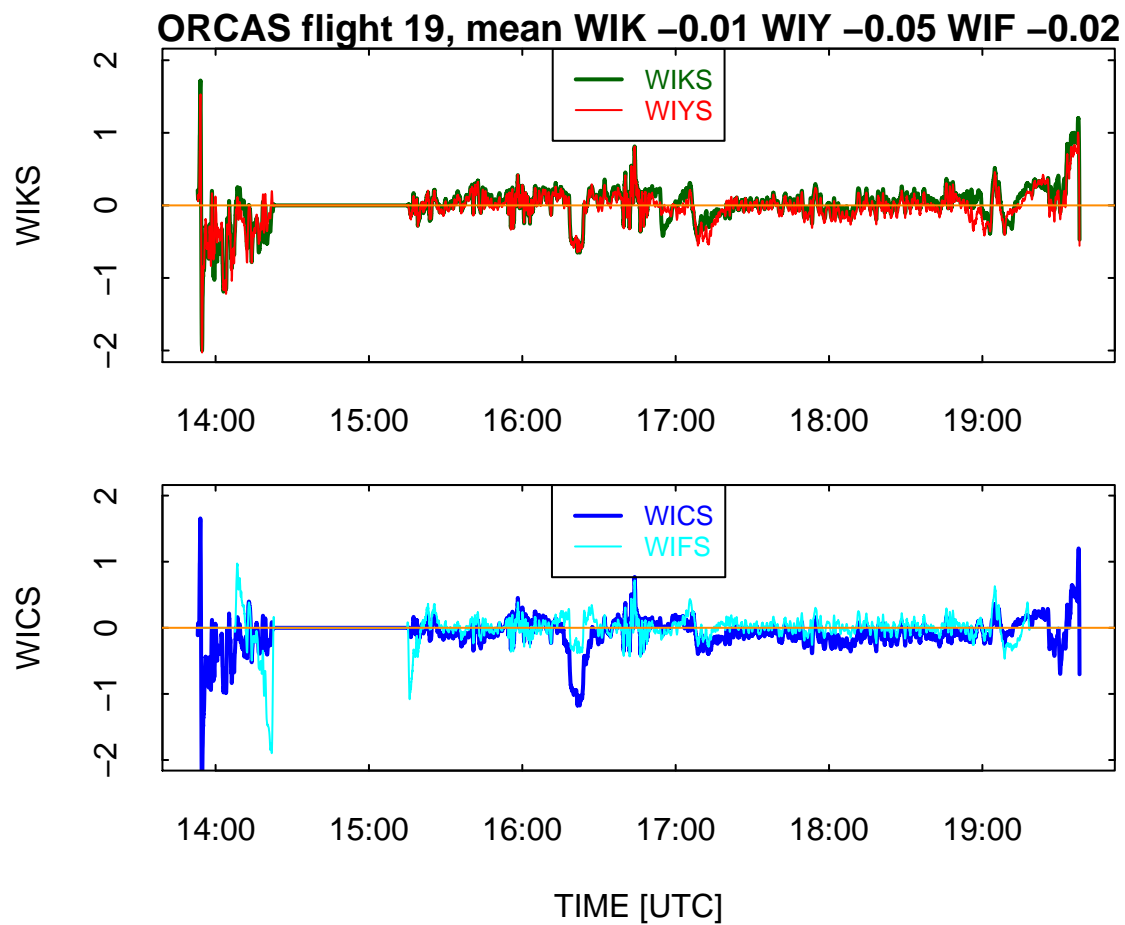


Figure 31: Plots for each ORCAS flight showing the four candidates for vertical wind.